SANDIA REPORT
SAND2026-18392
Printed March 2026

Sandia National Laboratories

Improbability of Post-Closure Criticality in Array of Transuranic Waste Containers after Compaction by Salt Creep at Waste Isolation Pilot Plant

Rob P. Rechard, Benjamin Reedlunn, James E. Bean, Jr.,
Brad A. Day, Lawrence C. Sanchez

Prepared by
Sandia National Laboratories
Albuquerque, New Mexico
87185 and Livermore,
California 94550

Issued by Sandia National Laboratories, operated for the United States Department of Energy by National Technology & Engineering Solutions of Sandia, LLC.

NOTICE: This report was prepared as an account of work sponsored by an agency of the United States Government. Neither the United States Government, nor any agency thereof, nor any of their employees, nor any of their contractors, subcontractors, or their employees, make any warranty, express or implied, or assume any legal liability or responsibility for the accuracy, completeness, or usefulness of any information, apparatus, product, or process disclosed, or represent that its use would not infringe privately owned rights. Reference herein to any specific commercial product, process, or service by trade name, trademark, manufacturer, or otherwise, does not necessarily constitute or imply its endorsement, recommendation, or favoring by the United States Government, any agency thereof, or any of their contractors or subcontractors. The views and opinions expressed herein do not necessarily state or reflect those of the United States Government, any agency thereof, or any of their contractors.

Printed in the United States of America. This report has been reproduced directly from the best available copy.

Available to DOE and DOE contractors from

U.S. Department of Energy
Office of Scientific and Technical Information
P.O. Box 62
Oak Ridge, TN 37831

Telephone: (865) 576-8401
Facsimile: (865) 576-5728
E-Mail: reports@osti.gov
Online ordering: http://www.osti.gov/scitech

Available to the public from

U.S. Department of Commerce
National Technical Information Service
5301 Shawnee Rd
Alexandria, VA 22312

Telephone: (800) 553-6847
Facsimile: (703) 605-6900
E-Mail: orders@ntis.gov
Online order: https://classic.ntis.gov/help/order-methods/


DEPARTMENT OF ENERGY
UNITED STATES OF AMERICA
NNSA
National Nuclear Security Administration

Improbability of Post-Closure Criticality in Array of Transuranic Waste Containers after Compaction by Salt Creep at Waste Isolation Pilot Plant

Rob P. Rechard
Applied Systems Analysis and Research Department 8844
Sandia National Laboratories,
Albuquerque, New Mexico 87185-0747

Benjamin Reedlunn
Materials and Failure Modeling Department 1558
Sandia National Laboratories
Albuquerque, New Mexico 87185-0840

James E. Bean, Jr.
Solid Mechanics Department 1554
Sandia National Laboratories
Albuquerque, New Mexico 87185-0840

Brad A. Day
Piru Associates, Inc.
Carlsbad, New Mexico

Lawrence C. Sanchez
Storage and Transportation Technology Department 8845
Sandia National Laboratories
Albuquerque, New Mexico 87185-0779

ABSTRACT

Based on the rationale presented, post-closure nuclear criticality is improbable when room closure compacts containers disposing transuranic (TRU) waste emplaced at the Waste Isolation Pilot Plant (WIPP), an operating repository in bedded salt in southeastern New Mexico. As described in the original WIPP certification, a qualitative estimate of the probability of post-closure criticality in TRU waste produced from atomic energy defense activities has been low either because remote-handled TRU waste canisters are neutronically isolated by the bedded salt or because the low fissile mass in an array of contact-handled TRU waste drums cannot be compacted sufficiently by room closure from salt creep. These situations are still valid for the majority of TRU waste that is disposed at WIPP without any disposal constraints, as updated herein. This report also qualitatively evaluates the probability of criticality after disposal of TRU waste in pipe overpack containers (POC) where every POC in a shipment may have the maximum 200 fissile gram equivalent of ^{239}Pu content. The probability of criticality for a disposal room filled with POCs is estimated during four representative phases of repository evolution: (1) a large salt block falls onto POCs in the first 20 years, (2) salt creep closes a disposal room in the first 1000 years without brine seepage and subsequent gas generation, which permits maximum compaction, (3) some brine seepage occurs into the closed room, which initiates consumption of the fiberboard (cellulose) impact absorber in the POC in the second 1000 years, and (4) full brine inundation of a room and consumption of all fiberboard thereafter. Salt-block fall in the first phase does not greatly disrupt three tiers of POCs. The compacted spacing of POCs in the later three repository conditions is calculated through high-fidelity, geomechanical modeling. Criticality evaluation of compacted 200-g ^{239}Pu spheres at the compacted spacing shows that neither 12-inch nor 6-inch POCs are critical after the first 1000 years, the second 1000 years, or thereafter as the sea of reflector material changes to represent the three repository conditions. Specifically, fiberboard and iron isolates ^{239}Pu while dry, and brine reduces the reactivity when a room is partially and fully inundated. Because POC behavior bounds behavior of other standard TRU waste containers, post-closure criticality caused by room closure compacting containers is omitted in the performance assessments for the 2019 and 2026 WIPP compliance re-certification applications to the US Environmental Protection Agency.

Keywords: post-closure criticality evaluation; features, events, and processes screening; transuranic radioactive waste disposal; safety assessment; performance assessment; Waste Isolation Pilot Plant

FOREWARD

The nuclear criticality calculations referenced within this document were originally published by Oak Ridge National Laboratory (ORNL) to meet the requirements of the US Environmental Protection Agency's (EPA) implementing regulation, 40 CFR §194.32(e)(3). The ORNL calculations are relied on to justify the exclusion of nuclear criticality impacting the Waste Isolation Pilot Plant (WIPP) disposal system during the post-closure regulatory timeframe. This justification is performed in accordance with EPA "reasonable expectation" standard of proof given in 40 CFR §191.13(b) for the post-closure timeframe. This report is being issued outside of Sandia National Laboratories' Nuclear Criticality Safety Program that is governed under 10 CFR 830 and US Department of Energy (DOE) Order 420.1C, Chg. 3 without receiving that program's concurrence or dissension of the conclusions within.

PREFACE AND ACKNOWLEDGEMENTS

EPA has regulatory authority for certifying the performance of WIPP in isolating radionuclides over the next 10 000 years against its long-term environmental standard specified in 40 CFR 191. The US Department of Energy (DOE), who is responsible for WIPP, has assigned Sandia National Laboratories (Sandia) to evaluate WIPP post-closure performance for EPA certification. Part of the performance assessment includes a formal analysis of all features, events, and processes (FEPs) that may impact WIPP isolation. EPA does not designate the post-closure criticality FEP for special consideration in 40 CFR 191. Rather, criticality is considered like all other FEPs.

The analysis reported here directly supports developing a rationale that post-closure criticality in an array of pipe overpack containers (POCs) is of low probability; thus, the criticality FEP is not necessary to include in WIPP performance assessments. The POC low-probability rationale is part of an overall probabilistic rationale for excluding post-closure criticality that is described in Appendix SCR of the 2026 WIPP Compliance Recertification Application to EPA, as managed by G. Ross Kirkes, Piru Associates.

This report updates the 2019 memorandum by R.P. Rechard, *Improbability of transuranic waste compaction by salt creep causing criticality in bedded salt repository*, which supported the 2019 Compliance Recertification Application to EPA. Importantly, discussion of the criticality control overpack (CCO) was moved to its own report. No new criticality calculations or POC container compaction simulations were conducted for this report. The 2019 calculational work and current analysis was supported by the Surplus Plutonium Disposition (SPD) program in the Material Management and Minimization Office within DOE. Paul E. Shoemaker, Sandia Senior Manager for Defense Waste Management Programs and Ronald Livingston, senior technical advisor to SPD program, provided coordination between the SPD program and Sandia for the 2019 memorandum. For this deliverable, Joshua Rutkowski, Sandia Manager International Safeguards and Engagements, was the liaison between the SPD program and Sandia.

The low-probability screening approach for the criticality evaluation uses geomechanical simulations to determine spacing for neutron transport modeling. Ben Reedlunn and James E. Bean, Jr. both from Sandia provided the geomechanical analysis, which is documented in several reports between 2018 and 2020. The most applicable is B. Reedlunn and J.E. Bean, Jr. *Simulations of pipe overpack container compaction at the Waste Isolation Pilot Plant*, SAND2019-12111. ORNL conducted the neutron transport modeling, which is documented in a B.D. Brickner, *Post-closure nuclear criticality evaluations involving 6- and 12-inch pipe overpack TRU waste containers at the Waste Isolation Pilot Plant*, ORNL/TM-2019/1222. Phil Jones and Mariah Garcia of Sandia conducted the internal review.

The POC evaluated here is managed by the WIPP management and operating (M&O) contractor for the US Department of Energy (DOE). The M&O is responsible for the nuclear criticality safety analysis in the Safety Analysis Report to the US Nuclear Regulatory Commission (NRC) that has shown criticality is incredible in POCs under normal and accident conditions. NRC has certified use of POCs in the TRUPACT-II package for transporting transuranic waste to WIPP. Furthermore, the M&O has shown criticality in POCs is incredible during normal and accident conditions at the WIPP facility prior to closure in the Design Safety Analysis report to DOE.

CONTENTS

I. Introduction 11
I.A. Low Probability Criterion for Screening Criticality Scenario 11
I.B. Approach for Low-Probability Rationale 12
II WIPP Disposal System 13
II.A Transuranic Waste 13
II.A.1. Legislative and Regulatory Constraints on TRU Waste Disposal 13
II.A.2. Surplus Plutonium 13
II.A.3. Projected TRU Contaminated Material 14
II.B. TRU Container Constraints 14
II.B.1. Type B Transportation Packages 15
II.B.2. CH-TRU Waste Type A Payload Containers 15
II.B.3. Pipe Overpack Containers 17
II.B.5. RH-TRU Type A Payload Canisters 18
II.C. Repository Design 19
II.C.1 Layout 19
II.C.2. MgO Engineered Barrier 20
II.C.3. RH-TRU Canisters in Repository Walls 21
II.D. Geologic Characteristics of WIPP Disposal Horizon 21
III. Roof Fall Modeling 22
III.A. Conceptual Model of Roof Fall 22
III.B. Results of Roof Fall on POCs 23
IV. Analysis of Room Closure from Salt Creep 25
IV.A. Compaction Analysis of POCs in 2009 25
IV.B. Conceptual Model for High-Fidelity Salt Creep Simulations 25
IV.B.1 Salt Creep Constitutive Model 25
IV.B.2. Geomechanical Model 25
IV.D. POC Deformed Irregular Array 26
IV.E. Closure Measure of Deformed Array 29
IV.F. Nearest Neighbor Measure of Deformed Array 29
IV.G. POC Concentration Measure of Deformed Array 29
V. Criticality Evaluation of POC Irregular Array 32
V.A. Computational Tool and Upper Subcriticality Limit 32
V.B. POC Conceptual Model for Criticality Evaluation 32
V.B.1. Plutonium Waste Form and Mass 32
V.B.2. Array Configuration and Fissile Shape 32
V.B.3. Hydrogenous Material Mixed with Fissile Material 33
V.B.4. Material in Reflector Box Surrounding Fissile Region 33
V.C. Criticality Evaluation of Closed Room without Brine 34
V.C.1. Waste Conditions Inside POC Pipe 34
V.C.2. Conditions Outside POC Pipe 34
V.C.3. Results for Closed Room without Brine 34
V.C.4. Sensitivity Cases 35
V.C.5. Correlation of POC Concentration with Neutron Tallies 35
V.D. Criticality Evaluation with Partially Degraded Fiberboard and Some Brine 35
V.D.1. Conditions near POC 35
V.D.2. Results with Some Brine Outside POC 36
V.E. Criticality Evaluation with Fully Degraded Fiberboard and Brine Inundation 36
V.F. Disturbed Conditions 36
VI. Analysis of CH and RH Containers 36
VI.A. Compaction of Standard CH Drums 36
VI.A.1. Drum Compaction as Homogeneous Block 37
VI.A.2. Compaction of Individual Standard Drums 37
VI.B. Comparison with Asymptotic Critical Concentration when Drums Compacted 39

VI.C. Standard CH-TRU Drum Behavior Bounded by POCs 39
VI.C. Fissile Concentration Less in Large Drums and Containers 40
VI.D. Neutronic Isolation of RH-TRU Canisters Placed in Room Wall 40
VI.E. RH-TRU Shielded Container Behavior Bounded by POCs 40
VII. Summary of Low-Probability of Criticality in Compacted Containers 41
VII.A. Constraints on POC Criticality 41
VII.A.1. Roof Fall in Room Filled with POCs 41
VII.A.2. Closure of Room Filled with POCs 41
VII.A.3. Material around POCs as Disposal Room Evolves over 10 000 Years 42
VII.A.4. Fiberboard and Iron Isolates POCs in Dry Repository 42
VII.A.5. Mixing 6-inch and 12-inch POCs 42
VII.A.6. Brine, Iron, and Fiberboard Isolates Degraded POCs 42
VII.A.7. Brine Absorbes Neutrons in Fissile Region of POCs 42
VII.B. Insufficient Compaction of Pu in Waste Drums and Boxes 42
VII.B.1. Low Pu Concentrations in Standard Waste Drums 42
VII.B.2. Low Pu Concentrations in Larger Drums and Standard Boxes 42
VII.C. Salt Isolates RH-TRU Canisters 43
VII.D. POC Behavior Bounds Shielded Container Behavior 43
References 45
Distribution 49

FIGURES

1. WIPP facility in southeastern New Mexico. 11
2. TRUPACT-II truck transport package for contact-handled TRU waste. 15
3. RH-TRU 72-B package for payload canister for remote-handled TRU waste, weighing up to 3.628 t.[49, Figure 1.1.1] 15
4. POC approved for use at WIPP: standard 12-inch POC is most common; standard 6-inch POC has only been used a few times and S200 POC has not yet been used.[15, Fig. 6] 18
5. Distribution of Pu fissile gram equivalent in POCs at WIPP (a) Repository; (b) Panel 1 (where Rooms 4, 5, and 6 only have waste in the southern drift corridor); and (c) Panel 2.[15, Figs 7,8,9;55] 19
6. TRU waste disposal area for WIPP repository currently consists of 6 filled panels and partially filled Panels 7 and 8; one equivalent panel in north central region, and proposed expansion of ≥2 replacement panels to west are yet to be filled.[15, Fig. 12] 20
7. Hypothetical arrangement of approved TRU waste containers in WIPP disposal room, which are stacked in up to three tiers.[54, Fig. 3;64, p. 26] 20
8. Placement of RH-TRU payload canisters in walls of disposal rooms. [15, Fig. 13] 21
9. Idealized model stratigraphy around WIPP disposal rooms in lower horizon (rooms in Panels 1, 2, 7, 8, and 10); and rooms in upper horizon (Panels 3, 4, 5, and 6) with elevations referenced to Clay G seam, which is at elevation 386 m, 652 m below surface at exploratory well ERDA-9.[15, Fig. 11;69;70, Fig. 1] 22
10. Conceptual model of large trapezoidal-shaped salt block that detaches at Clay G seam and falls onto 3 tiers of stacked POCs; ~1905-kg MgO sacks are not included in model. [15, Fig. 14] 22
11. Roof fall of large trapezoidal-shaped salt block in Room 4 of Panel 7 in lower horizon at WIPP in November 2016.[15, Fig. 18;23, Fig. 2-5] 23
12. Negligible deformation and disruption of containers after large trapezoidal-shaped block falls onto room filled with POCs emplaced in a hexagonal array, where blue is flanged inner pipe, and red is top and bottom plywood spacer; fiberboard impact absorber and outer 55-gallon overpack drums are present but removed in visualization.[15, Fig. 19;23, Fig. 3-1] 24
13. Slice of WIPP disposal room filled with POCs (a) ideal hexagon array of 57 POCs in one tier at emplacement (171 POCs in 3 tiers—1.85 kg $^{239}Pu/m^2$), (b) deleted 12 half POCs in a tier (153 POCs in 3 tiers—1.66 kg $^{239}Pu/m^2$) in geomechanical model. 26
14. Deformed inner pipes of standard POCs emplaced as hexagonal array in representative WIPP disposal room closed by salt creep; red elements represent plywood spacers, which stabilize the pipe, but many disappear because they are deleted when they splinter and fail; the outer drum, fiberboard impact absorber, and bedded salt stratigraphy are included in analysis but removed in visualization.[15, Fig. 20;23, Fig. 3-2] 27

15. Deformed centerlines, centers, and centroids of inner pipes of standard POC at 1000 y with friction coefficient of 0.5 for Clay F and Clay G layers. 28
16. Horizontal and vertical closure at mid-height and mid-width of WIPP disposal room filled with 6-inch and 12-inch POCs in lower repository horizon (rooms in Panels 1, 2, 7, 8, and 10).[15, Fig. 21;23;82] 29
17. Distribution of distance between POC centroids at 1000 years based on nearest neighbor: 12-inch POC with 31.8-cm average/23.3-cm minimum; and 6-inch POC with 23.7-cm average/10.9-cm minimum.[23] 29
18. Distribution of POC concentration in 0.75 m sphere about each centroid at 1000 years. 30
19. Number of centroids in 0.75-m radial sphere at each of 153 POC locations in 2.15-m disposal room segment in lower repository horizon. 31
20. Mineral form of highly enriched Pu only influences criticality limits for sphere when mixture is severely under moderated.[12, Fig. 7;13, Fig. 8] 32
21. Three material regions of MCNP criticality model, with dimensions of Region 2 defined by maximum extent of the centroid coordinates of the POC inner pipe. 33
22. Critical limits for ^{239}Pu sphere mixed with water, Salado brine, polyethylene, and volume mixture of 25% polyethylene, 74% fluid (water or Salado brine), and 1% beryllium as used in detailed ORNL MCNP criticality model.[12, Fig. 10] 33
23. Critical ^{239}Pu sphere radius in water, Salado brine, polyethylene, and volume mixture of 25% polyethylene, 74% fluid (water or Salado brine), and 1% beryllium compared to radius of 6-inch and 12-inch POCs.[12, Fig. 10] 33
24. Cellulose mass remaining throughout repository for undisturbed scenario in 100 simulations of Replicate 2 (mean and median displayed is based on all 3 replicates of CRA-2019).[15, Fig. 24] 34
25. Multiplication factor for irregular compacted array of 6-inch and 12-inch POCs without brine influx as represented by infinite number or 153 spheres in WIPP room segment with 200 g ^{239}Pu moderated with water/plastics and reflected by salt or iron oxide/fiberboard (where fiberboard set at either 100% or 60% of initial mass).[15, Fig. 25;84, App. G] 35
26. Neutron tallies at one horizontal slice for 12-inch POC shows k_{eff} dominated by several locations on right side of room that qualitatively correspond to high concentration in Fig. 20a. 35
27. Multiplication factor for irregular compacted array of 6-inch and 12-inch POCs vary between 0.96 and 0.91, respectively, for conditions without brine, between 0.90 and 0.85 for conditions with some brine between POCs, and between 0.40 and 0.36 for conditions with brine inside POC.[15, Fig. 27;84, App G] 36
28. Deformation of disposal room with 55-gallons drums emplaced as hexagonal array in upper horizon closed by salt creep;[63, Fig. 3-16] thin shelled drums of carbon steel, which quickly shell buckle and shear, are removed as simulation progresses. 38
29. Eulerian porosity when represented as homogeneous block and hexagonal/triangular arrangements of discrete 55-gallon drums in room segment in upper horizon closed by salt creep without gas generation.[63, Fig. 3-15] 39
30. Critical limits for plutonium mixed with materials potentially present near 55-gallon drums at 20% porosity saturated with Salado brine.[12, Fig. 35;14, Fig. 28]. 39
31. Neutron communication between RH-TRU payload canisters emplaced horizontally in salt with contents modeled as 1-D planar neutron source in MCNP and absorption by stainless-steel payload canister omitted. [15, Fig. 28] 40
32. Neutron communication between RH-TRU shielded containers emplaced in disposal rooms with contents modeled as 1-D planar neutron source in MCNP when neutron absorption by carbon-steel drum omitted.[15, Fig. 29] 41

TABLES

I. Projected fissile mass at closure for WIPP certifications....13
II. Average mass anticipated in waste destined for WIPP in recent performance assessments....14
III. Volume and counts for TRU containers emplaced at WIPP through April 2019.[14, Table VI]....16
IV. Plutonium transportation and administrative limits for CH-TRU containers shipped to WIPP.[14, Table V;52, Table 3.1-1]....17
V. Plutonium transportation limits for RH-TRU 72-B shipping RH-TRU waste to WIPP.[14, Table VII;55]....19
VI. MgO mass and volume emplaced in WIPP Rooms....21
VII. Composition of WIPP Salado and Castile brines.....22
VIII. Rationale that rockfall and salt-creep compaction of POC, drums, and boxes in disposal rooms has low probability of causing criticality at WIPP.[14, Table XI]....44

ACRONYMS AND INITIALISMS

CCA	Compliance Certification Application
CCO	criticality control overpack (container)
CH-TRU	contact-handled transuranic (waste)
CRA	Compliance Re-certification Application
DOE	US Department of Energy
EPA	US Environmental Protection Agency
FEP	features, events (natural and anthropogenic phenomena of short duration), and processes (natural phenomena of long duration)
FGE	fissile gram equivalent
HalfPACT	Half Transuranic Package Transporter packaging
MCNP	Monte Carlo N-Particle transport code
NRC	US Nuclear Regulatory Commission
PA	performance assessment; the process of assessing whether a system or component meets a set of performance criteria. For US, the process is a stochastic simulation; the system is a deep geologic repository disposal system; the performance criteria are the long-term measures in the EPA post-closure environmental standard 40 CFR 191
POC	pipe overpack container
RH	remote-handled (transuranic waste)
TDOP	ten-drum overpack
TRU	transuranic radionuclide (waste)
TRUPACT-II	Transuranic Package Transporter Model 2 packaging
SLWB2	standard large waste box, model 2
SWB	standard waste box
US	United States
USL	upper subcriticality limit
WIPP	Waste Isolation Pilot Plant (repository in southeastern New Mexico for TRU waste from atomic energy defense activities)

I. INTRODUCTION

The possibility of sufficient fissile mass causing a self-sustained neutron chain reaction is unlikely after closure of the Waste Isolation Pilot Plant (WIPP), an operating repository in bedded salt owned by the United States (US) Department of Energy (DOE) for disposal of wastes containing transuranic (TRU) radioisotopes (Fig. 1), As described in the initial WIPP certification, the low probability of sustained neutron chain reaction (hereafter, succinctly referred to as criticality) in TRU waste was readily demonstrated because of the usually low fissile mass in each contact-handled container. For example, the maximum fissile mass is 325 fissile gram equivalent (FGE) ^{239}Pu in the TRUPACT II Type B transportation packaging. Other reasons included the neutronic isolation of mostly fissile uranium in remote-handled containers when disposed and the natural tendency of fissile solute to disperse after release from degraded containers, as discussed in 2001 and summarized in 2015.[1-3]

The content of contact-handled containers, however, have expanded to include containers with higher maximum allowable fissile mass, such as pipe overpack containers (POCs) with an allowable mass of 200 FGE ^{239}Pu per container, and criticality control overpack (CCO) containers with an allowable mass of 380 FGE ^{239}Pu per container.[4] Furthermore, all CCOs and POCs may contain the maximum fissile content when transported. Thus, for example, TRUPACT II package may transport 5320 FGE in 14 CCOs or 2800 FGE in 14 POCs versus a total of 325 FGE per container with other container types.

Hence, a renewed evaluation of the improbability of a critical mass and concentration being assembled after WIPP closure has been undertaken for TRU waste that includes diluted surplus plutonium material that meets waste acceptance criteria for contact-handled waste.[5;6] The evaluation supports excluding post-closure criticality in performance assessments used to demonstrate compliance of WIPP with standards of the US Environmental Protection Agency (EPA),[7]

The criticality screening update is divided into five parts: evaluation of the post-closure criticality potential from (1) geomechanical compaction, through salt creep, of TRU waste drums, boxes, and POCs emplaced in disposal rooms; (2) compaction of CCOs in disposal rooms,[8;9] (3) fissile mobilization then deposition in other parts of disposal system from hydrologic and geochemical processes;[10] (4) a summary of the low risk of post-closure criticality as demonstrated by combining the low probability and low consequences of post-closure criticality,[11] and (5) neutronic criteria after fissile deposition in geologic media.[12-14] This paper discusses the first part.

This paper in combination with companion reports demonstrates that the possibility of criticality is remote in a geologic setting. Hence, post-closure criticality was omitted from the performance assessments for the 2019 and 2026 Compliance Re-certification Applications (CRA-2019[7;15] and CRA-2026, respectively) to EPA, which are the latest required periodic compliance demonstrations with EPA performance criteria since WIPP opened in 1999.

The 2026 analysis conducted a PA for an interim state repository with 2 additional panels in the disposal area (12 panels total), designated CRA-26-12P, and conducted a PA for the final state repository with 9 additional panels (19 panels total), designated CRA-26-19P. The evaluation reported here is for post-closure criticality in a disposal room filled with POCs at their maximum fissile mass and so is unaffected by the total inventory and number of panels, so herein we usually refer to CRA-2026 inclusively. However, the inventory of radionuclides or waste components must be explicit.



Fig. 1. WIPP facility in southeastern New Mexico.

I.A. Low Probability Criterion for Screening Criticality Scenario

An analysis to examine the probability for criticality in the post closure time frame (i.e., post-closure criticality evaluation[a]) is conducted within the probabilistic regulatory framework for radioactive waste disposal defined by EPA in Title 40 Code of Federal Regulations Part 191 (40 CFR 191). In 40 CFR 191,[16-18]

[a] We refer to the analysis here as a criticality evaluation to show the improbability of criticality in the post-closure timeframe when humans are absent. We only use the term nuclear criticality safety analysis in §II.B and §V.A when we wish to connote a rule-based approach to show criticality is incredible when humans are present during operations.

EPA defines the process of assessing whether the WIPP radioactive waste disposal system meets its regulatory criteria as a performance assessment, where a performance assessment (PA) answers three basic questions:[19] What features, events, and processes (FEPs) and scenarios formed from these FEPs may occur in the disposal? What is the probability of each FEP or scenario? What are the consequences in terms of the performance criteria of each FEP or scenario?[b]

EPA establishes three guiding criteria for omitting FEPs, such as criticality, from the PA in Appendix C of 40 CFR 191:[16;17] and in 40 CFR §194.32,[18;21] (1) regulatory fiat; (2) low consequence; and (3) low probability of occurring. In regards to the probability criterion, EPA explicitly states[16,App. B;17, App. C] "…performance assessments need not consider categories of events or processes that are estimated to have less than one chance in 10,000 of occurring over 10,000 years." However, direct estimation of a numerical probability is not required. EPA also allows a reasoned qualitative low-probability rationale that argues against the likelihood of criticality in the underground after closure, as done here, based on arguments that room compaction cannot sufficiently concentrate an array of fissile ^{239}Pu spheres.

I.B. Approach for Low-Probability Rationale

Support for a low-probability rationale in the closed WIPP repository depends upon constraints developed from two types of quantitative modeling: geomechanical phenomenological modeling and neutron/photon transport criticality modeling.

The waste is emplaced subcritical, and geomechanical modeling evaluates the feasibility of room closure from salt creep assembling fissile material into a critical array configuration. To establish the evolution of POC spacing in the disposal room after WIPP closure, four phases of repository behavior are modeled: (1) roof fall in the first 20 years or so; (2) room closure compacting containers to the maximum extent up to 1000 years without brine present; (3) a transitional phase in the second 1000 years with influx of some brine that partially saturates room porosity and initiates some POC degradation; and (4) a final phase with influx of sufficient brine to saturate room porosity and complete POC degradation. The configuration changes in the first two phases (hereafter described as repository conditions). The availability of moisture changes in the last three phases (hereafter described as hydrologic regimes).

Geomechanical and hydrologic changes can occur simultaneously, and WIPP PAs allow a full range of possibilities. But by separating geomechanical deformation from brine inflow for FEP screening, we avoid including gas generation[22] from metal corrosion and cellulose degradation and, thereby, allow for the maximum compaction of POCs, which is the phenomenon we are most interested in for evaluating the potential for criticality in this paper.

Geomechanical modeling estimates a reasonable, representative deformed irregular array of POCs compacted by room closure for the first two repository conditions,[23] with a wide range of container arrangements; not a worse case container arrangement. This paper also greatly expands upon previously published modeling of room closure and compaction of standard TRU drums conducted for the initial 1996 Compliance Certification Application (1996 CCA) to EPA.[1;3;24]

In the compaction analysis, conservative estimates of some parameters are used, and conservative initial and boundary conditions are set, but they are not set at extreme physical situations and parameter values. This choice is consistent with the EPA concept of reasonable expectation, [16;17] which connotes a flexible standard of proof and use of central estimates when encountering unknowns.

The nuclear criticality modeling evaluates whether the compacted arrays of containers with plutonium are sufficient to promote nuclear criticality. For criticality modeling, we model the maximum fissile content of a container (e.g., 200 FGE ^{239}Pu for a POC) confined in a spherical configuration at the final coordinate positions of the centroids of each POC in the deformed, irregular array. Bounding estimates of material present about the container are used (e.g., 60% of cellulosic fiberboard in POC).

To conceptually organize the low probability rationale, the probability of criticality is notionally conceived as the sum of the probability of room closure through salt-creep sufficiently compacting three categories of containers disposing TRU waste: (1) POCs for contact-handled transuranic (CH-TRU) waste, (2) various drum and box containers for CH-TRU waste, and (3) canisters and shielded containers for remote-handled transuranic (RH-TRU) waste.

II WIPP DISPOSAL SYSTEM

II.A Transuranic Waste

II.A.1. Legislative and Regulatory Constraints on TRU Waste Disposal

In its radiation protection standard 40 CFR 191,[16;17] EPA designated material contaminated with TRU

[b] The US Nuclear Regulatory Commission (NRC) defines a scenario as[20] "a well-defined, connected sequence of FEPs that can be thought of as an outline of a possible future condition…" Within the WIPP Project, a scenario is a set of FEPs that outlines a possible future condition but does not include the timing or ordering of events and processes. Once a mathematical model of the disposal system is developed, timing and order of events and processes are introduced.

isotopes with an activity > 3.7 MBq/kg (>100 nCi/g) and half-life of >20 years as TRU waste that requires deep geologic disposal. Two types of TRU waste destined for WIPP are defined in the *Waste Isolation Pilot Plant Land Withdrawal Act*:[25] (1) CH-TRU waste with an external dose rate <0.56 μSv/s (200 mrem/h), and (2) RH-TRU waste with > 0.56 μSv/s but < 2.8 mSv/s (1000 rem/h).

The *WIPP Land Withdrawal Act* codifies limits on TRU waste disposal at WIPP,[25, §9] based on prior social-political agreements between the State of New Mexico and DOE (in the Consultation and Cooperation Agreement and the Stipulated Agreement and their negotiated modifications in the 1980s).[18;26;27] TRU waste disposed at WIPP must have been produced from atomic energy defense activities. The activity of RH-TRU is limited to < 190 PBq (5.1 MCi) with a concentration < 0.85 PBq/m^3 (23 Ci/L). WIPP is limited to 175 564 m^3 (6.2×10^6 ft^3) of which 7079 m^3 may be RH-TRU.

II.A.2. Surplus Plutonium

In response to the 1991 Strategic Arms Reduction Treaty (START I) with Russia, DOE identified ~50 metric tons (t) of Pu surplus to defense needs in a 1996 Programmatic Environmental Impact Statement (51.4 t are specifically identified below).[28] In 1997, DOE committed to fabricate 34 t non-pit Pu into mixed oxide (MOX) fuel to be consistent with plans in Russia. The other ~17.4 t was to be immobilized and included (a) 3.2 t Pu residues and scraps already disposed in POCs as CH-TRU at WIPP, (b) 1.1 t of miscellaneous Pu, (c) 7.1 t of Pu from weapon pits, and (d) 6.0 t non-pit Pu unsuitable for producing MOX fuel. Disposition of 7.1 t pit Pu and 6.0 t non-pit Pu (13.1 t total) in lanthanide borosilicate glass and 34 t of Pu as spent MOX fuel was included in the license application for the proposed Yucca Mountain (YM) repository.[29;30]

After the YM repository was suspended in 2010, DOE decided (1) in 2011 to dispose the 1.1 t of miscellaneous surplus Pu;[31] and (2) in 2012 to dispose the 6.0 t of non-pit Pu[32] as CH-TRU at WIPP by diluting the plutonium oxide (PuO_2) and placing the diluted mixture in CCOs. The 3.2-t Pu residues in POCs, and 7.1 t of surplus Pu in CCOs are considered in CRA-2019 (Table I).[7]

Because DOE cancelled plans to produce MOX fuel, DOE has decided to dispose the 34 t of surplus Pu material at WIPP in CCOs.[5;6;33] Disposal of 6 t and 34 t of surplus Pu as CH-TRU in CCOs is considered in CRA-2026 and discussed in a companion report.[9] The 3.2-t Pu residues in POCs is the focus of this paper.

For the 1996 CCA, the projected ^{239}Pu mass in CH-TRU was 13 t. The projected ^{239}Pu content in CH-TRU dropped after the 1996 CCA. The projected ^{239}Pu content is 14 t in CRA-2019 with the addition of 6.0 t of non-pit surplus Pu. However, the projected 15 500 FGE of CH-TRU is still less than the 16 700 FGE in the 1996 CCA (Table I). The ^{239}Pu enrichment of CH-TRU is 90% for the 1996 CCA and has remained near that value in the intervening years.

Table I. Projected fissile mass at closure for WIPP certifications

Radioisotope	1996 CCA[34;35]		CRA[b]-2004[36;37]		CRA[c]-2009[38-40]		CRA-2014[41]		CRA-2019[42]		CRA-26-19P[43]	
	CH (kg)	RH (kg)	CH (kg)	RH (kg)	CH (kg)	RH (kg)	CH (kg)	RH (kg)	CH (kg)	RH (kg)	CH (kg)	RH (kg)
Uranium												
^{233}U	860	16	130	3.5	16	5.3	10	42	11	1.8	37	13
^{234}U	75	6.9	45	6.0	49	0.83	34	52	77	1.6	118	3.2
^{235}U	5 900	2 100	610	440	2 000	33	4 000	31 000	2 100	860	807	945
^{238}U	120 000	31 000	73 00	390 000	81 000	880	104 000	88 000	117 000	9 300	321 230	10 400
Enrichment ^{233}U+^{235}U	4.9%	6.5%	1.0%	0.11%	2.5%	4.1%	3.7%	26%	1.8%	8.4%	0.26%	8.4%
Plutonium												
^{238}Pu	15	0.09	73	0.16	86	0.30	35	0.34	55	1.3	92	1.4
^{239}Pu	13 000	170	11 000	87	8 200	47	9 100	120	14 000	68	67 200	73
^{240}Pu	920	22	470	7.5	630	4.4	740	35	1 400	14	4 860	20
^{241}Pu	2.2	0.13	5.0	0.23	4.9	0.04	6.3	0.14	18	0.44	5.6	0.08
^{242}Pu	310	0.04	6.8	0.12	19	0.32	420	1 600	38	4.0	73	6.1
^{239}Pu fissile kg mass equivalent[b]	16 700	1 560[c]	11 200	370[c]	9 590	73.0	11 800	20 300[c]	15 500	624[c]	67 900	697[b]
Enrichment ^{239}Pu	90%	88%	95%	92%	92%	90%	88%	6.5%	90%	78%	92%	73%

[a] Inventory mass differs somewhat for EPA-requested PABC-2004 analysis for evaluating CRA-2004[37]

[b] Pu fissile mass equivalence is the mass of ^{239}Pu plus factors for other fissionable masses: specifically, 0.113·^{238}Pu, 0.0225·^{240}Pu, 2.25·^{241}Pu, 0.0075·^{242}Pu, 0.9·^{233}U, 0.643·^{235}U, 0.015·^{237}Np, 0.0187·^{241}Am, 34.6·^{242m}Am, 0.0129·^{243}Am, 15·^{245}Cm, 0.5·^{247}Cm, 45·^{245}Cf, and 90·^{251}Cf.[44,Table XVI;45,§5.2]

[c] Pu fissile kg mass equivalence for RH-TRU derives primarily from 0.643 ^{235}U

Both ^{239}Pu enrichment and FGE varies more for RH-TRU. The ^{239}Pu FGE derives mostly from ^{235}U; the ^{239}Pu

and ^{240}Pu contribute only a small amount to FGE. The projected ^{235}U mass was 5.9 t in CH-TRU and 2.1 t in RH-TRU for the 1996 CCA.

The corresponding ^{235}U enrichment at emplacement was 4.9% for CH-TRU and 6.5% for RH-TRU waste. The projected uranium ^{235}U enrichment of CH-TRU at emplacement has remained <4.9% since the 1996 CCA (Table I) but does increase to 4.5% for CRA-2019 after ^{239}Pu decay over 10^4 years. The RH-TRU uranium enrichment is 8.4% in CRA-2019 and remains fairly constant over 10^4 years.

II.A.3. Projected TRU Contaminated Material

CH-TRU waste primarily consists of a variety of debris contaminated with TRU radionuclides, including organics (e.g., cellulose material—such as paper, cardboard, laboratory tissues, wood, cloth—rubber, and plastics), and inorganics (e.g., iron and aluminum alloys, equipment, glass, firebrick, ceramics, cement, and soils) (Table II).

II.B. TRU Container Constraints

Because of the robust capability of geologic disposal in general, and the WIPP salt repository, in particular, few technical constraints exist on waste management and emplacement beyond the constraints for transportation (i.e., if the waste can be shipped it can be disposed provided social-political agreements in the *WIPP Land Withdrawal Act* are met[c]). The disposal function of TRU waste containers is to allow retrieval of waste during operations. None of the containers used at WIPP act as an engineered barrier to release after repository closure.

The transportation limits on waste containers set the boundary conditions for the potential for criticality inside the package. Transportation packaging is the primary barrier between the radioactive material being transported and radiation exposure to the public and workers. The type of transportation packaging used is determined by the total radioactive hazard presented by the material within the packaging. Four basic types of packaging are used in the US: Excepted, Industrial, Type A, and Type B (49 CFR 173.400). Excepted and Industrial packaging can be used to transport radioactive materials at very low concentration when of limited hazard to the public and the environment.

Type A packaging is designed to protect and retain its contents under normal conditions of transport (NCT) and maintain sufficient shielding to limit radiation exposure to handling personnel (10 CFR 71.71, Subpart F). Three Type A certified payload containers used at WIPP are considered in this paper (1) various drums and boxes for CH-TRU waste, (2) POCs for CH-TRU waste, and (3) payload canisters and shielded containers for RH-TRU waste.

Table II. Average mass anticipated in waste destined for WIPP in recent performance assessments.

Material	CRA-2019[42] CH (t)	CRA-2019[42] RH (t)	CRA-26-19P[43] CH (t)	CRA-26-19P[43] RH (t)
Waste				
Organics				
Cellulose	4 100	170	4 480	177
Plastics	5 320	414	5 610	305
Rubber	1 090	51.2	1 130	47.1
Solidified Organics	5 280	3.7	3 750	9.6
Organic Total	15 790	638.9	1497	538.7
Inorganic				
Fe Metal	14 100	1 330	21 200	943
Al Metal	513	43.6	431	65.6
Other Metal	827	157	1 600	143
Solidified Inorganic	12 100	36.1	12 400	36.8
Other Inorganic	5 970	4 490	6 920	458
Cement	1 760	2.08	1 196	16.0
Soils	4 990	19.0	4 750	10.7
InorganicTotal	40 260	6 078	48 497	1673
Waste Total	56 050	6 717	63 470	2 212
Packaging				
Cellulose	1 470	0	6 010	0
Plastic	2 830	468	4 610	1 090
Lead	0	13 800	113	4.96
Steel	31 200	16 500	0	9 050
Package Total	35 500	30 738	52 700	13 900
Emplacement/Operation				
Cellulose	224		302	
Plastic	1550		2 460	
Rubber	4.8		4.85	
Emplace Total	1779		2 770	
Totals				
Fe	45 300	17 830	73 900	14 840
Cellulose	5790	170	10 800	177
Plastic	9700	882	12 680	1 400
Rubber	1170	57	1250	52
*Cements**	8 880	3.5	8 590	17.4
Total Material	93 329	37 455	129 670	26 250

*Cements are also included in solidified inorganic, solidified organic, and other inorganic material categories.

II.B.1. Type B Transportation Packages

Radioactive materials shipped in Type A payload containers at WIPP are subject to specific radioactivity limits in 10 CFR 71, by the US Nuclear Regulatory Commission (NRC), and 49 CFR 173.435, by the Department of Transportation. If the limits are exceeded, the material or the Type A payload container must be shipped in a Type B package. In addition to the normal conditions of transport described for Type A containers,

[c] Although this rule-of-thumb applies to most containers used at WIPP, CCOs have constraints on contents beyond those imposed by transportation, as discussed in a companion report.[9]

a Type B package must (1) provide shielding from radiation, (2) dissipate the heat generated by the waste, and (3) withstand a hypothetical accident condition (HAC) without releasing radioactive material (where testing includes 9-m drop onto unyielding surface, 1-m drop onto 15 cm steel bar, and 800 °C fully engulfing fire for 30 minutes).

Currently, five NRC-approved Type B packagings exist for shipping TRU waste: TRUPACT-II (Transuranic Package Transporter Model 2),[46] HalfPACT,[47] TRUPACT-III (only for large standard waste boxes), RH-TRU 72-B,[48] and 10-160B. Up to three TRUPACTs or three HalfPACTs are transported on a truck to WIPP (Fig. 1 and Fig. 2). The Type B fissile and total mass limits depend upon the Type A container shipped (Table III).

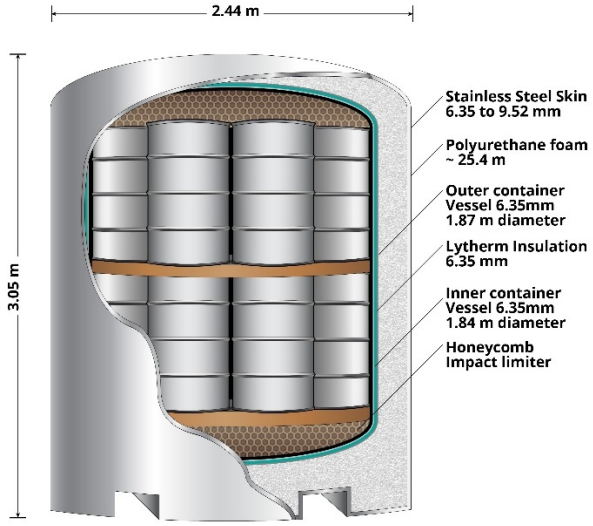

Fig. 2. TRUPACT-II truck transport package for contact-handled TRU waste.

One RH-TRU 72-B package is transported on a truck (Fig. 3).

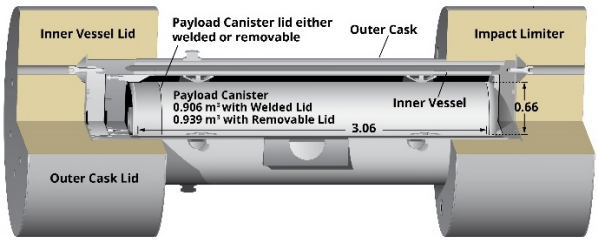

Fig. 3. RH-TRU 72-B package for payload canister for remote-handled TRU waste, weighing up to 3.628 t.[49, Figure 1.1.1]

II.B.2. CH-TRU Waste Type A Payload Containers

About 53.9% of CH-TRU waste payload containers are standard 55-gallon drums (Table III). The 55-gallon drums are bound together in hexagon-shaped packs of seven for transportation and disposal (one container surrounded by six containers). The TRUPACT-II holds 2 seven packs (14 drums) (Fig. 2). The HalfPACT holds one seven pack.

About 19.5% of CH-TRU containers are 100-gallon drums that often contain machine super-compacted mixed waste from the advanced mixed waste treatment project (~60 MPa compression, which is >>14.7 MPa lithostatic pressure at WIPP). The 100-gallon drums are bound together as 3 packs for shipment in the HalfPACT (see §II.C.1). Also, 85-gallon short and 85-gallon tall drums are available (Table III).

Another 7% of CH-TRU containers are standard waste boxes (0.94 m high, 1.3 m wide, 1.8 m long) (see §11.C.1). Two standard waste boxes are shipped in TRUPACT-II and one in HalfPACT. The ten-drum overpack (TDOP) is ~ 4% of the CH-TRU containers at WIPP.

As licensed by NRC,[46;47] TRUPACT-II and HalfPACT packages generally have a transportation limit of 325 FGE ^{239}Pu when drums or boxes are shipped, if the waste is not machine compacted, contains ≤ 1 wt % of beryllium (Be/BeO), and has no reported ^{240}Pu (Table IV).[50, Table 1;51] The limit increases somewhat if up to 25 g of ^{240}Pu is also in the container (380 FGE ^{239}Pu in Table IV). Except for POCs and CCOs, the limit decreases to 250 FGE ^{239}Pu if the waste is mechanically compacted. Except for POCs, the limit decreases to 100 FGE ^{239}Pu if the waste has >1 wt % Be/BeO. CCOs may not transport waste with >1 wt % Be/BeO.

No credit is given for the ability of standard drums and boxes to maintain fissile separation after an accident. Rather, the mass limit is based on the maximum mass that can remain subcritical as an optimally moderated sphere in a water/polyethylene mixture.

The fissile limit of any one drum is further limited to 200 Pu FGE (Table IV). The limit is not based on transportation accident analysis but rather is an administrative limit imposed to ensure that an array of drums or boxes (uncompacted) is subcritical without

requiring explicit nuclear criticality safety analysis and controls during storage at generator sites and WIPP. Thus, if a drum is at the administrative maximum of 200 FGE ^{239}Pu, the TRUPACT-II and HalfPACT packagings can carry only a little more than one drum of fissile material (i.e., 200 g + 125 g =325 FGE maximum for TRUPACT-II); the other drums in the transportation package must be dunnage.

Table III. Volume and counts for TRU containers emplaced at WIPP through April 2019.[15, Table VI]

Payload Container				Bundle for Shipping and Disposal			Disposed Amount				
Type	Unit Volume[52] (m^3)	Admin Fissile Limit[a] (g)	Unit Fissile Concen (g/m^3)	Ship Config	Waste Volume (m^3)	Approx Dispose Area (m^2)	Count[b]	(%)	Volume[b,c] (m^3)	(%)	Total (%)
CH											
55-Gallon Drum	0.216	200	930[d]	7-Pack	1.50	3.52	94 924	53.9	20 503.58	27.0	26.8
				2, 7-Pack	3.00						
85-Gallon Drum Tall	0.324	200	620	4-Pack	1.33	3.23	5	0.0	1.62	0.0	0.0
85-Gallon Drum Short	0.315	200	640	2, 4-Pack	2.52	3.48	0	0	0	0	0
100-Gallon drum	0.385	200	520	3-Pack	1.15	3.21	34 290	19.5	13 201.65	17.4	17.2
Standard Waste Box (SWB)	1.880	325	170	One	1.35	2.33	13 155	7.5	24 731.40	32.6	32.3
Standard Large Box 2 (SLB2)	7.380	325	44	One	7.38		232	0.1	1 712.16	2.3	2.2
Ten-Drum Overpack (TDOP)	2.16[e]	325	150	One	2.05	3.43	6 685	3.8	14 439.60	19.0	18.9
12-inch Pipe Overpack	0.0488	200	4 100[f]	7-Pack	0.34	3.52	25 937	14.7	1 265.73	1.7	1.7
				2, 7-Pack	0.68						
6-inch Pipe Overpack	0.0120	200	16 670	7-Pack	0.09	3.52	0	0	0	0	0
				2, 7-Pack	0.18						
S100 Pipe Overpack[g]	0.00163	200	122 700	7-Pack	0.011	3.52	846	0.5	1.38	0.0	0.0
				2, 7-Pack	0.022						
S300 Pipe Overpack[g]	0.00269	200	74 350	7-Pack	0.019	3.52	56	0.0	0.15	0.0	0.0
				2, 7-Pack	0.038						
Criticality Control Container	0.00206[h]	380	184 470	7-Pack	0.014	3.52	0	0	0	0	0
				2, 7-Pack	0.029						
CH Total							176 130	100.0	75 857.23	100.0	
RH											
Canister, removable lid	0.939	245	261	One	0.94		701	94.0	658.24	97.1	0.9
Canister, welded lid	0.906	245	270	One	0.91		18	2.4	16.31	2.4	0.0
Shielded Container	0.117[i]	200	1709	3-Pack	0.35	3.31	27	3.6	3.16	0.5	0.0
RH Total							746	100.0	677.71	100.0	
Total							176 876		76 534.98		100.0

[a] See Tables V and VII; minimum Pu FGE reported.
[b] Latest available from https://www.wipp.energy.gov/general/GenerateWippStatusReport.pdf ; values similar to September 2019 in Ref[6, Table 5-1]
[c] Volume based on inner volume of inner most container, as used for assessing against *WIPP Land Withdrawal Act* limits.
[d] Disposed average FGE concentration in containers other than POCs is ~92 FGE/m^3 i.e., 16.1 (CH and RH in CRA 2019 from Table I) –6.0 t (CCO estimate)–3.2 t (POCs))/(76 534.98 –(1265.73+1.38+0.15) m^3); if other containers are all 0.21 m^3 drums then 19.3 FGE per drum.
[e] Ten-drum overpack can overpack 55-gal and 85 gal drums or be loaded directly; directly loaded volume is 4.37 m^3; 2.16 m^3 volume is when overpacking ten 55-gallon drums.
[f] Disposed average FGE concentration in POCs is ~2 528 FGE/m^3 (i.e., 3.2 t /1267.26 m^3) where 3.2 t =119.5 FGE per POC ×26 839 POCs from Fig. 5 and 1265.73 m^3 total volume mentioned in §II.B.3.
[g] Neutron source disposal.
[h] Volume of 0.00206 m^3 is used for transporting surplus Pu;[52] total volume available in a CCO is 0.0128 m^3.
[i] Volume in authorized 30-gallon inner drum.

Table IV. Plutonium transportation and administrative limits for CH-TRU containers shipped to WIPP.[15, Table V;53, Table 3.1-1]

Conditions		Type A Payload Containers	Type B Container[c]		
				TRUPACT-II	HalfPACT
			Administrative FGE Pu+2σ[a,b] (g)	Transport FGE Pu+2σ (g)	Transport FGE Pu+2σ (g)
Not machine Compacted ≤ 1 wt. % Be/BeO	No ^{240}Pu	Drums (55-gal: two 7-packs or one 7-pack;	200	325	325
		85-gal short: two 4-packs in TRUPACT-II	200	325	
		85-gal tall: one 4-pack in HalfPACT	200		325
		100-gal: one 3-pack in HalfPACT)	200		325
	5 g ^{240}Pu	(Similar FGE container limits for 55-gal, 85-gal short, 85-gal tall, and 100-gal)"	200	340	340
	15 g ^{240}Pu	(Similar drum packaging configurations)	200	360	360
	25 g ^{240}Pu	(Similar drum packaging configurations)	200	380	380
	No ^{240}Pu	Standard Waste Box (SWB) &	325	325	325
	5 g ^{240}Pu	Standard Large Box 2 (SLB2)[d]	325	340	340
	15 g ^{240}Pu		325	360	360
	25 g ^{240}Pu		325	380	380
		Ten-Drum Overpack (TDOP): one in TRUPACT	325	325	
		Shielded Container: one 3-pact in HalfPACT	200		325
		Pipe Overpack Container (POC) (Std 12-in; Std 6-in; S100, S200, S300): two 7-packs or one 7-pack	200	2800	1400
		Criticality Control Overpack (CCO): two 7-packs or one 7-pack	380	5320	2660

[a] Standard deviation (σ) is from measurement uncertainty of fissile material.
[b] In the future, the limit for drums may be raised to 325 FGE ^{239}Pu, like ten-drum overpacks, because an array of drums is far from critical.
[c] Operational nuclear criticality safety analysis allows more fissile mass in containers but transportation limits are bounding.[51, §9]
[d] SLB2 container uses TRUPACT-III packaging, which has the same fissile limits as TRUPACT-II except it cannot transport machine compacted TRU waste or TRU waste with > 1 wt. % Be/BeO.
[e] 200 FGE ^{239}Pu allowed in POC provided Be/BeO mechanically bound to fissile material.
[f] Containers with machine compacted waste may not be emplaced next to each other in a disposal room.
[g] 380 FGE ^{239}Pu allowed in CCO provided ≤ 2 kg plastic in machine compacted TRU waste.[46;47]

II.B.3. Pipe Overpack Containers

POCs, which consist of a 55-gallon drum with an interior stainless-steel pipe (Fig. 4), have been used to transport the 3.2-t surplus Pu to WIPP. As of April 2019, POCs represented 14.7% of the 176 130 CH-TRU waste containers disposed at WIPP (Table III).[6, p. 29] Conceivably, POCs could be used to transport standard CH-TRU waste when more than one standard drum might approach the 200 FGE ^{239}Pu limit of a drum and 325 FGE ^{239}Pu limit of TRUPACT-II (Table IV). However, the more economical CCO would likely be used in the future.

During a transportation accident, a POC can maintain fissile separation as demonstrated to the NRC; hence, each POC in a shipment can be at the administrative maximum 200 FGE ^{239}Pu; thus, TRUPACT-II and HalfPACT can transport 2800 FGE ^{239}Pu and 1400 kg FGE ^{239}Pu, respectively, when the waste is compacted or >1 wt.% Be/BeO (Table IV).

Although POCs represent ~15% of the CH-TRU containers, the POCs represent a small portion of the total volume of TRU waste disposed. As the volume is currently measured using the inner most container, 75 857 m^3 has been disposed at WIPP (Table III), of which ~1270 m^3 is in POCs, or 1.7%. Of this 1270-m^3 disposed, standard 12-inch POCs represents 99.9 %vol; hence, the average fissile concentration is ~2500 g ^{239}Pu /m^3 (i.e., 3.2 t/1270 m^3).

The space between the inner pipe and 55-gallon outer drum is filled with fiberboard (Fig. 4), which protects the waste during transportation and handling accidents but provides little structural support at slow strain rates from salt creep. Without structural support, the 12-inch inner stainless-steel pipes are susceptible to shell buckling (like the bellows of an accordion) since the diameter-to-thickness ratio is 55 and length-to-diameter ratio is 2.

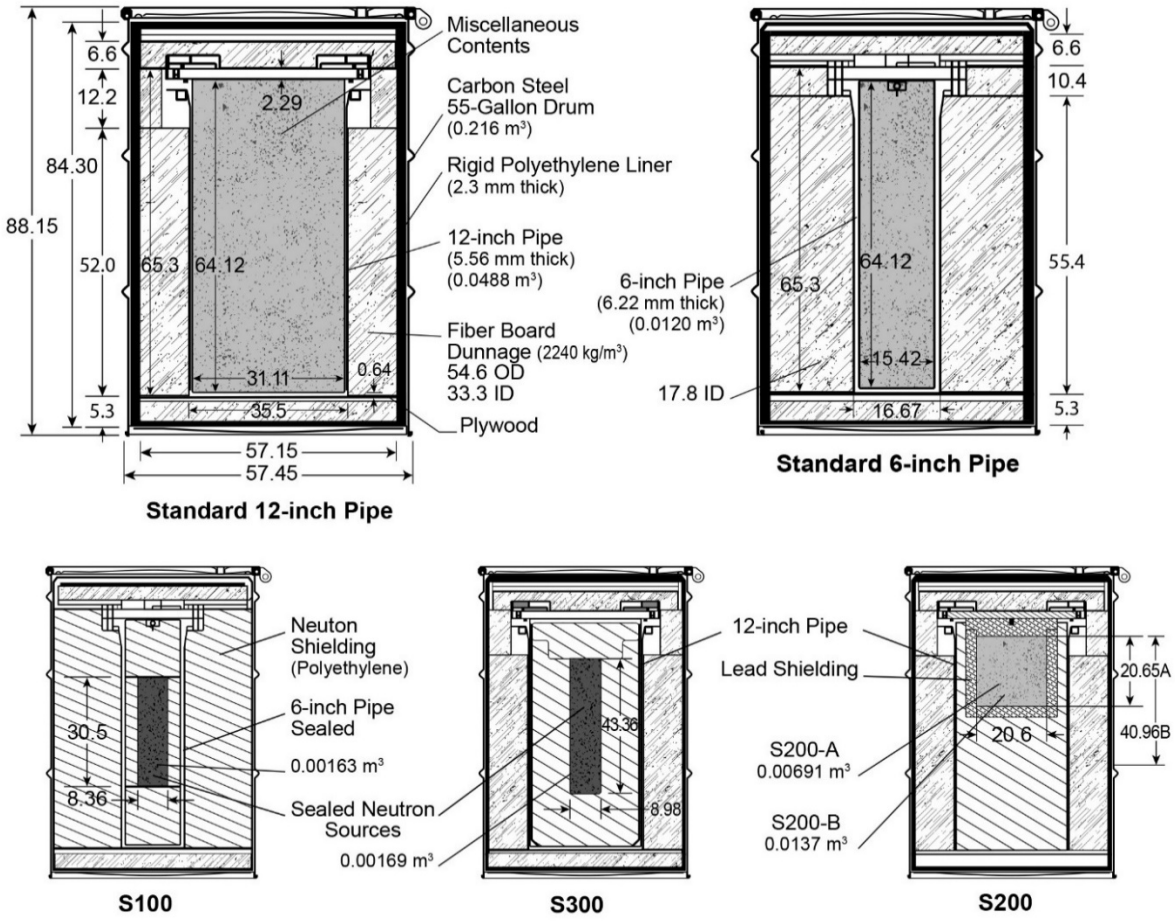

Fig. 4. POC approved for use at WIPP: standard 12-inch POC is most common; standard 6-inch POC has only been used a few times and S200 POC has not yet been used.[15, Fig. 6]

The 6-inch POC is susceptible to column buckling because the diameter-to-thickness ratio is 24.0, length-to-diameter ratio is 4.0, and the fiberboard impact absorber provides insufficient lateral structural support as the plywood spacers splinter when the roof initially touches POCs. Other POCs use either a variation of the 12-inch (0.1%) or the 6-inch POC (0.01%) and, thus, are adequately represented by the two standard POCs in the criticality analysis.

Pu residue and some scraps from cleaning up the former Rocky Flats plant in Colorado was sent to WIPP and placed in Panel 1 in ~17 000 POCs (Fig. 5b and Fig. 5c).[54] Since that time ~9 800 more POCs from various sources have been sent to WIPP (Fig. 5). The 26 800 containers contain ~3.2 t of ^{239}Pu, which is part of the 51.4 t of surplus Pu discussed in §II.A.3. The average content is 119.5 g ^{239}Pu per POC (Fig. 5).

II.B.5. RH-TRU Type A Payload Canisters

RH-TRU waste is shipped in either (a) 3-pack of carbon-steel payload containers with lead shielding in the HalfPACT; or (b) a carbon steel or 304 stainless-steel payload canister in the RH-TRU 72-B package (Fig. 3). The RH payload canister has 66 cm outer diameter, 306 cm outer height including 21 cm lid, and 0.635 cm thickness; the internal volume is 0.939 m^3 for a removable lid and 0.906 m^3 for welded lid.[49;52] As licensed by NRC,[48] the RH payload canister has a 370 FGE ^{239}Pu limit provided ≥ 25 g of ^{240}Pu is present and ≤ 1% Be/BeO is present (Table V).[50, Table 3] As of April 2019, 2005 containers in 715 RH-TRU payload canisters (i.e., ~3 containers per canister) have been placed in room walls (see §II.C.3).

Shielded containers can maintain fissile separation during an accident, but this capability has not been demonstrated to the NRC. Hence, the Pu limit for the HalfPACT is set at the default value of 325 FGE ^{239}Pu (Table IV). In addition, individual shielded containers have an administrative 200-FGE ^{239}Pu limit (Table IV).

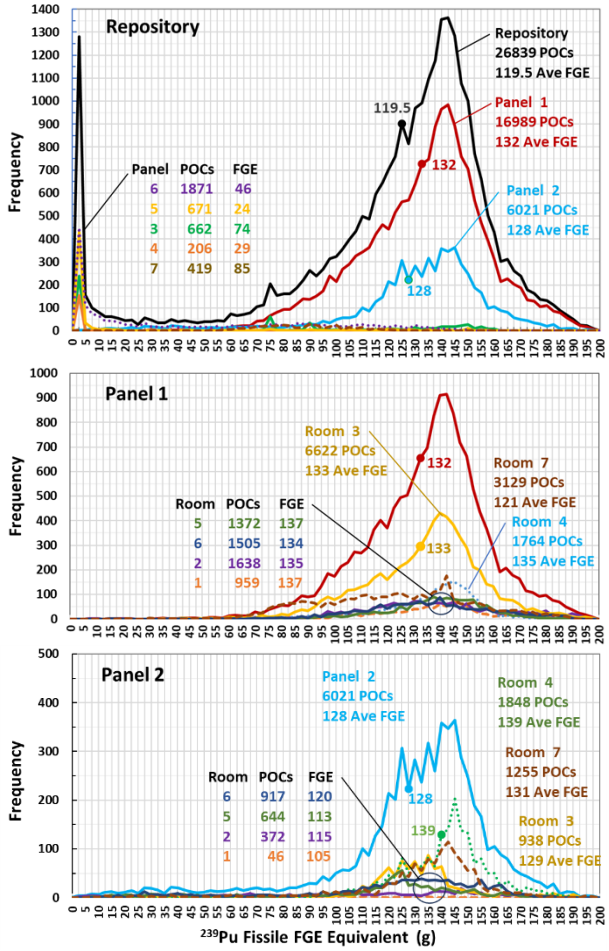

Fig. 5. Distribution of Pu fissile gram equivalent in POCs at WIPP (a) Repository; (b) Panel 1 (where Rooms 4, 5, and 6 only have waste in the southern drift corridor); and (c) Panel 2.[15, Figs 7,8,9;55]

The shielded container placed inside a 30-gallon drum has a disposal volume of 0.117 m^3 (Table V). The shielded container has 58.4-cm outer diameter, 90.8-cm outer height, and 0.437 cm thickness (8-gauge carbon steel). The thickness of the lead shielding placed between the outer carbon steel of the drum and inner carbon steel shell is 2.54 cm. In the future, however, other versions may have 5.08 cm and 7.62 cm of lead to provide more shielding.

Although handled and emplaced in disposal rooms like CH-TRU drums, the 0.117 m^3 volume and disposed activity are counted against the RH-TRU waste statutory limits of 7079 m^3 and 190 PBq (§III.C.2).

As an aside, 27 shielded containers with 2.54-cm lead shielding have been shipped from Argonne National Laboratory (ANL). For the 27 drums, the average ^{239}Pu is 0.533 FGE (and derives mostly from ^{235}U at 11.7% enrichment). The 0.533 FGE is far from the 200 FGE allowed.

Table V. Plutonium transportation limits for RH-TRU 72-B shipping RH-TRU waste to WIPP.[15, Table VII;56]

Conditions		RH-TRU 72-B FGE $^{239}Pu+2\sigma$ (g)
Not machine compacted ≤ 1 wt. % Be/BeO	No ^{240}Pu	315
	5 g ^{240}Pu	325
	15 g ^{240}Pu	350
	25 g ^{240}Pu	370
Not machine compacted > 1 wt. % Be/BeO are chemically bound to Pu		305
Not machine compacted > 1 wt. % Be/BeO not chemically bound to Pu		100
Machine compacted ≤ 1 wt. % Be/BeO		245
Machine compacted > 1 wt. % Be/BeO		Unauthorized

II.C. Repository Design

II.C.1 Layout

In the original WIPP repository design, the excavated disposal region was divided into eight panels plus two slightly smaller equivalent panels composed of the 4 central connecting drifts for a total of 4.42×10^5 m^3 (Fig. 6).[57, Table 3.1-1] All the openings for disposal in the panel are rectangular in cross section (10.06 m wide, and 3.96 m high), and a full panel is ~4.61×10^4 m^3.[57, Table 3.1-1] Ideally, 3636 hexagonal prism columns can be placed in a full panel.[58, Figure DATA-B-11]

Because of the accidental release of ^{241}Am, ^{239}Pu, and ^{240}Pu in 2014 that contaminated some of the underground[59] and lack of ceiling maintenance with rock-bolts during the subsequent 3-year shutdown, DOE has abandoned the southern equivalent panel to keep worker hazards low.[60] Also, packing inefficiencies occurred in the disposal area. Finally, EPA and State of New Mexico have allowed DOE to redefine the TRU waste disposal volume to include only the inner most waste container; not the entire container volume. Hence, at least two replacement panels will be necessary[61] and up to seven additional panels have been proposed. The expansion does not change the maximum TRU waste volume of 175 564 m^3 (6.2×10^6 ft^3) authorized for disposal in the *Waste Isolation Pilot Plant Land Withdrawal Act*.[25]

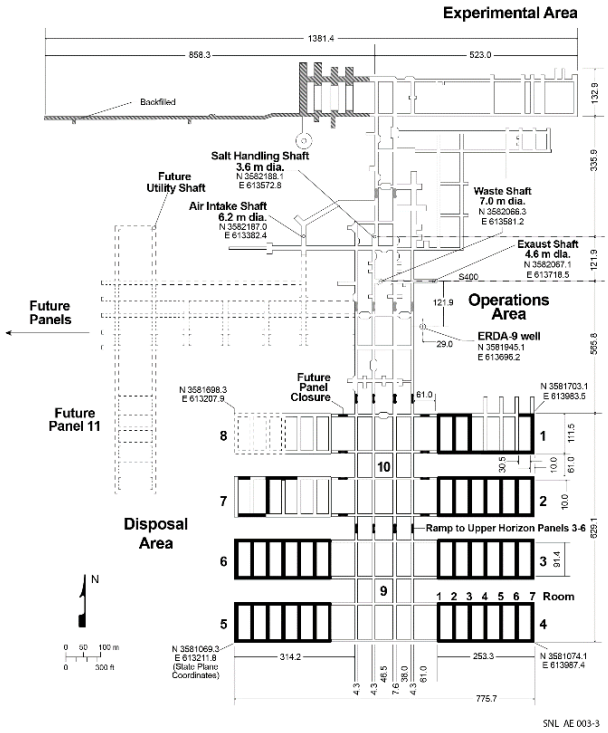

Fig. 6. TRU waste disposal area for WIPP repository currently consists of 6 filled panels and partially filled Panels 7 and 8; one equivalent panel in north central region, and proposed expansion of ≥2 replacement panels to west are yet to be filled.[15, Fig. 12]

A full panel is divided into 7 rooms. The new panels and rooms are the same size but the salt pillar between the panel and access drift have increased from 61 m to 122 m and the pillars between panels have increased from 61 to 91.5 m.

The volume of a room is 6585 m^3, including the connecting drifts to form a square bracket shape.[d] Although this room definition is important for tracking disposal room contents, analysis for creep closure (and gas generation)[22] usually model a straight room segment (to avoid three dimensional effects) that is 91.4 m long with 3644 m^3 volume [62] and disposes 6804 drums (i.e., six 7-packs across the room segment width, stacked in 3 tiers, and 54 rows of 7-packs down the straight room segment length).[54] Herein, we refer to the straight room segment rather than an entire disposal room. The contents of standard waste drums occupy 40.4% of the initial room segment volume (using 0.216 m^3 per inner drum volume—Fig. 4). The drums and their contents occupy 47.4% (1728 m^3—using 0.2359 m^3/drum, based on outer diameter of drum ribs). The average initial room porosity (including the porosity in typical waste) is about 91%.[63]

Standard waste boxes, 85-gallon tall drums, 100-gallon drums and ten-drum overpacks are also used, but the container groupings all occupy about the same areal footprint because they are all transported in either TRUPACT-II or HalfPACT (Table V). Only the 3-pack shielded container, whose areal footprint is limited to keep the lead shielding mass reasonable for HalfPACT, and the rectangular Standard Large Box 2 (SLB2), which is transported in TRUPACT-III, change the normal packing (Fig. 7).

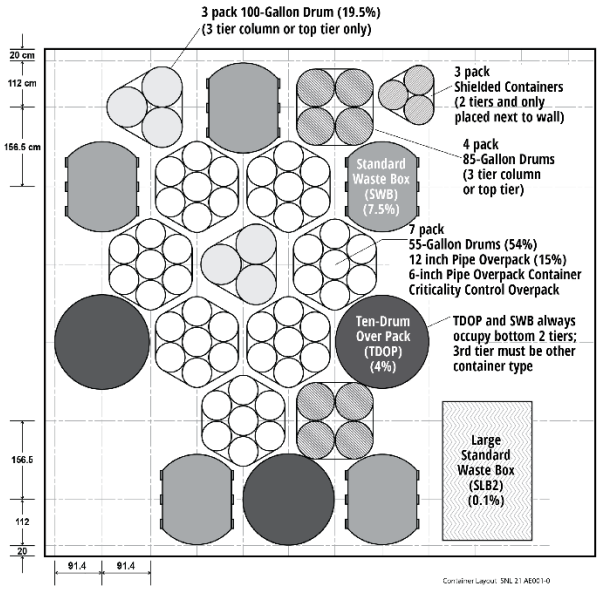

Fig. 7. Hypothetical arrangement of approved TRU waste containers in WIPP disposal room, which are stacked in up to three tiers.[54, Fig. 3;64, p. 26]

II.C.2. MgO Engineered Barrier

Part of the disposal room volume is filled with sacks of magnesium oxide (MgO). Brine seepage hydrates the MgO engineered barrier and combines with available CO_2 to form hydromagnesite ($Mg_5(CO_3)_4(OH)_2 \bullet 4H_2O$) in order to prevent forming carbonic acid (H_2CO_3*), which would enhance dissolution of radionuclides. The hydromagnesite, which may eventually convert to thermodynamically stable magnesite ($MgCO_3$), also buffers the brine chemistry between pH 8.8 and 9.

The MgO mass emplaced is adjusted for every batch of containers that is disposed. The mass (m_{MgO}) is calculated assuming a one-to-one correspondence between CO_2 produced and six times mass of carbon in

[d] Ideally 10 908 55-gallon drums can be placed per full room (i.e., 3636 stacks/7 rooms or 519.4 stacks/room with twenty-one 55-gallon drums/stack).[58, Figure DATA-B-11] In actuality, 40 rooms were filled with 18 317 stacks at the end of 2014. Hence, on average, 458 stacks were placed per room for an equivalent of 9 616 drums/room (88% of maximum). Thus, the contents of standard waste drums occupy 31.5% (2077 m^3) of the initial full room volume (using 0.216 m^3 per inner drum volume). The drums and their contents occupy 34.5% (2268 m^3–using 0.2359 m^3/drum).

waste cellulose (m_{cell}) ($C_6H_{10}O_5$), rubber (m_{rub}), and factor of 1.7 times mass of plastics (m_{plstc}) with a safety factor (f_{MgO}^{safety}):[65;66]

$$m_{MgO} = 6 f_{MgO}^{safety} \left(m_{cell} + m_{rub} + 1.7 m_{plstc} \right) \bullet \frac{40.3 \text{g/mole MgO}}{162 \text{ g/mole cellulose}} \quad (1)$$

Between 1996 and 2000, f_{MgO}^{safety} of Eq(1) was set at 1.95 and applied to Panel 1. Between 2001 and February 2008, f_{MgO}^{safety} was set at 1.67 and applied to Panels 2, 3, and 4.[67] After February 2008, f_{MgO}^{safety} has been set at 1.2.[68] The MgO mass (m_{MgO}) using f_{MgO}^{safety} of 1.2 translates to ~91 kg MgO/POC for a POC filled with an average of 9.94 kg plastic and 33.91 kg cellulose/rubber.[55]

Table VI. MgO mass and volume emplaced in WIPP Rooms

	Room-Segment MgO Mass per 7 Rooms in a Panel[a,b] (metric tons—t)		
Panel	**Ave**	**Max**	**Min**
1	354	624	123
2	527	569	383
3	508	566	367
4	512	581	370
5	416	518	269
6	260	411	130
7	149	307	32
Overall	389	624	32
Panels 5,6,7	275	518	32
	Porous Volume[c] (m^3)		
Overall	180 (4.9%)	289 (7.9%)	15 (0.4%)
Panels 5,6,7	127 (3.5%)	240 (6.6%)	15 (0.4%)

[a] Query of the WIPP Waste Data System on 3 August 2023
[b] Adjusted by ratio of full volume to straight segment volume (i.e., 6585m^3/3642 m^3)
[c] Assumes 3600 kg/m^3 grain density and 40% MgO porosity

For a room filled with 6804 POCs, the granular MgO occupies 7.9% (287 m^3) of initial room volume of 3642 m^3, based on a MgO grain density of 3600 kg/m^3 and emplaced porosity of 40%. In comparison, a standard CH-TRU drum has an average of ~14 kg cellulose, which requires 25 kg of MgO per drum and translates to 2.2.% (79 m^3) of initial disposal room volume.

Although some rooms in Panels 1 through 4 containing POCs, might have up to 7.9% of the disposal room volume backfilled with sacks of MgO, the current emplaced average in Panels 5, 6, and 7 is 3.5% (Table VI). Thus, a 1905 kg polypropylene sack of MgO is placed on every other column of containers in a typical room.

II.C.3. RH-TRU Canisters in Repository Walls

RH-TRU waste may now come in lead shielded containers and be disposed in the rooms (Table III), but originally, all RH-TRU waste was to arrive in RH-TRU 72-B payload canisters and be disposed in 4.6-m boreholes in the repository walls (ribs) (Fig. 8).

Boreholes have been drilled to accommodate the frequency of RH-TRU shipments: 194 RH-TRU canisters emplaced in Panel 4, 264 canisters in Panel 5, 239 canisters in Panel 6, and 18 canisters in Panel 7. No more than 32 boreholes have been drilled in a room wall and borehole centerlines are spaced no less than 2.4 m apart (Fig. 8).

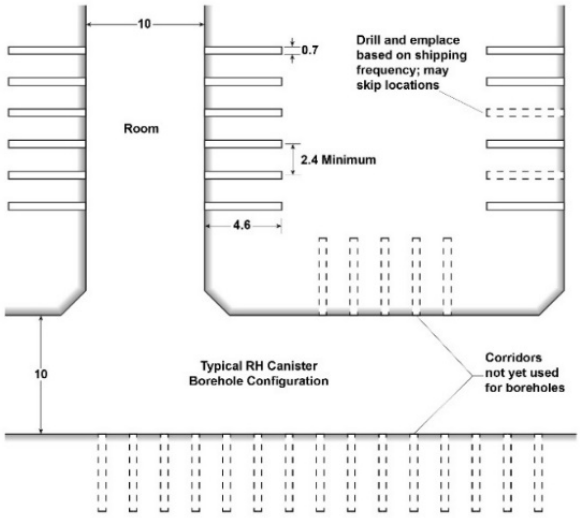

Fig. 8. Placement of RH-TRU payload canisters in walls of disposal rooms. [15, Fig. 13]

II.D. Geologic Characteristics of WIPP Disposal Horizon

The WIPP underground facility is constructed in the 600-m thick Salado Formation between a depth of 652 and 658 m (Fig. 9). The Salado consists of nearly horizontal (<1° regional dip) halite (NaCl), argillaceous halite, and interbeds of clay and anhydrites ($CaSO_4$) near the repository upper and lower horizons (Fig. 9).[1, Fig. 4]

Fractured anhydrite strata and the disturbed halite around the disposal rooms allow intergranular Salado brine to enter the rooms as the salt slowly creeps and encapsulates the TRU waste.

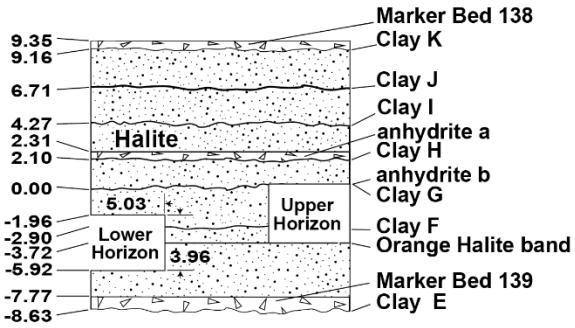

Fig. 9. Idealized model stratigraphy around WIPP disposal rooms in lower horizon (rooms in Panels 1, 2, 7, 8, and 10); and rooms in upper horizon (Panels 3, 4, 5, and 6) with elevations referenced to Clay G seam, which is at elevation 386 m, 652 m below surface at exploratory well ERDA-9.[15, Fig. 11;69;70, Fig. 1]

Within the land-withdrawal boundary of the WIPP disposal system, one exploratory borehole (WIPP-12) intersected a pressurized brine reservoir in a fractured anhydrite layer of the Castile Formation, which underlies the Salado Formation.[34, Appendix DEL, Section 7.5] Consequently, WIPP PAs assume (1) a pressurized brine reservoir beneath a portion of the repository, and (2) Castile brine enters the repository through a new exploratory borehole in the next 10^4 years. Castile brine has substantially less magnesium, potassium, boron, and chloride compared to intergranular Salado brine at the repository horizon (Table VII). Chloride and boron decrease the criticality potential of the fissile/solution mixture. Hence, the initial Castile brine composition is conservatively used for criticality evaluations in §V.[e]

Table VII. Composition of WIPP Salado and Castile brines.

Constituent	Concentration (mM or mole/m³) Salado (Weeps)[a]	Castile (ERDA-6)[b]
Sodium (Na^{+1})	3530	4870
Magnesium (Mg^{+2})	1020	19
Potassium (K^{+1})	467	97
Calcium (Ca^{+2})	14	12
Boron ($B(OH)_4^{-1}$)	158	63
Chloride (Cl^{-1})	5860	4800
Sulfate (SO_4^{-2})	177	170
Bromine (Br^{-1})	27	11
Bicarbonate (HCO_3^{-1})	16	16

[a] Intergranular fluids of Salado Formation[71;72]
[b] Early experimental well drilled to Castile Formation[71;73]

[e] The brine composition of Salado brine changes somewhat as it reacts with steel/lead in containers in the disposal rooms.[71] However, the fluid composition before and after reaction with the Castile brine is similar except for a large increase in Mg^{+2} (from 19 mM to 387 mM), from the MgO emplaced in the rooms.[71] Solid MgO can act as a reflector, but Mg^{+2} in solution has little influence on the reactivity.[14, Table V & Fig. 4]

III. ROOF FALL MODELING

III.A. Conceptual Model of Roof Fall

As documented for operations,[51;74] an infinite array of uncompacted POC containers, each with 200 g FGE ^{239}Pu and reflected by 63.5 cm of MgO on the top of a stack of 3 containers[f] and 300-cm salt above the MgO and bottom of containers, is subcritical at emplacement in the disposal rooms because of the initial, uncompacted spacing between drums.

During the first 20 years of room closure, some roof fall may occur along with rapid salt creep to mostly fill/close the unfilled void space in the room (Fig. 10). Salt blocks may fall but the air gap between the waste drums and ceiling is a maximum of 1.3 m (prior to salt creep diminishing the distance) for a room in the lower horizon such that the block cannot accelerate much before is strikes and settles on top of the containers.

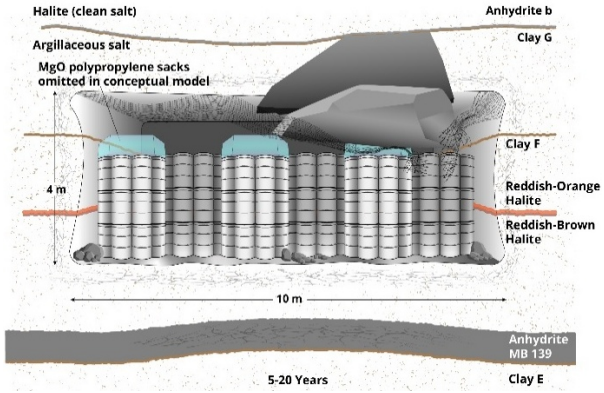

Fig. 10. Conceptual model of large trapezoidal-shaped salt block that detaches at Clay G seam and falls onto 3 tiers of stacked POCs; ~1905-kg MgO sacks are not included in model. [15, Fig. 14]

Furthermore, MgO polypropylene sacks on top of POC stakes easily burst and cushion the impact. Granted, super compacted TRU waste disposed in 100-gallon drums do have sufficient strength to prop up a small area of a room, but in the case of roof fall the 3-packs of rigid 100-gallon drums would likely cause the salt block to break apart, which would decrease the impact energy.[75]

A discrete roof fall model was constructed to evaluate the potential of roof fall clustering POCs and, thereby, creating a reactive POC configuration prior to full compaction from salt creep. Six conservative assumptions are made to construct a reasonably bounding case for 12-inch and 6-inch POCs:[23]

[f] The 63.5-cm MgO thickness equates to ~231 kg cellulose/POC as follows: $M_{POC}^{MgO} = V_{POC}^{MgO} \rho_{MgO}^{grain} \left(1 - \phi_{final}^{room}\right)$ =(57.45²·63.5cm³/3)·(3600 kg/m³)·(1−0.08).

1. A large trapezoidal-shaped block is modeled to emulate the largest roof fall observed at WIPP, which occurred in Room 4 of Panel 7 (Fig. 11). The large rock detached at Clay G seam and so a thicker block is unlikely (Fig. 9 and Fig. 10). Modeling a trapezoidal-shaped block thick on one side and thin on the other imparts some moment and uneven impact with the potential to push and cluster the containers to one side of the room.
2. The large block is not allowed to fracture and break in pieces (i.e., the constitutive model for the salt block allows plastic/creep deformation but not fracturing of the salt), such that all the energy of the impact is absorbed by the assembly of POCs.
3. Each of the three stacked tiers of POCs are offset 2.54 cm in the same direction to promote minor instability and facilitate shifting and toppling the POCs.
4. Roof fall occurs immediately such that salt creep has not reduced the gap between the ceiling and the POCs.
5. Polypropylene sacks holding MgO are omitted to conservatively increase the free fall distance and avoid dissipating any impact force (Fig. 12).
6. POCs are modeled empty (i.e., structural resistance of TRU waste inside a POC is not included).

Four components of the POC (internal stainless-steel pipe, its plywood stabilizer on the top and bottom, fiberboard impact absorber around pipe, and outer 55-gallon carbon steel drum shell) are discretely modeled with individual elastic-plastic-failure material models with several conservative assumptions: (1) the plywood strength was reduced 80% to promote greater inner pipe movement; (2) the stainless steel and carbon steel use the minimum annealed yield strength; and (3) the carbon steel 55-gallon drum, fiberboard, and stainless-steel inner pipes use constitutive parameters based on slow strain rates; these materials are stronger and stiffer at the high strain rates that would occur from the rock block impact. Defining container strength as a function of strain rate would more accurately model impact conditions but would also increase the stability of the POC array.



Fig. 11. Roof fall of large trapezoidal-shaped salt block in Room 4 of Panel 7 in lower horizon at WIPP in November 2016.[15, Fig. 18;23, Fig. 2-5]

III.B. Results of Roof Fall on POCs

In the roof-fall simulations, the entire length of the trapezoidal salt block detaches from the roof. Although the shape imparts a small rotation, the block lands mostly flat. It bounces slightly then settles on top of the drum ensemble. The impact dents some of the 55-gallon outer drums (not shown), causes the pipes (blue) to sway back and forth slightly but results in <5% pipe deformation, without changing the disposed configuration of the POCs (Fig. 12). Because of the bounding conditions selected, large salt block falls shortly after disposal are not likely to cause collapse and major clustering of drums in one area of a disposal room prior to later salt creep. Hence, a criticality evaluation of small clusters of POCs prior to salt creep compaction is not necessary.

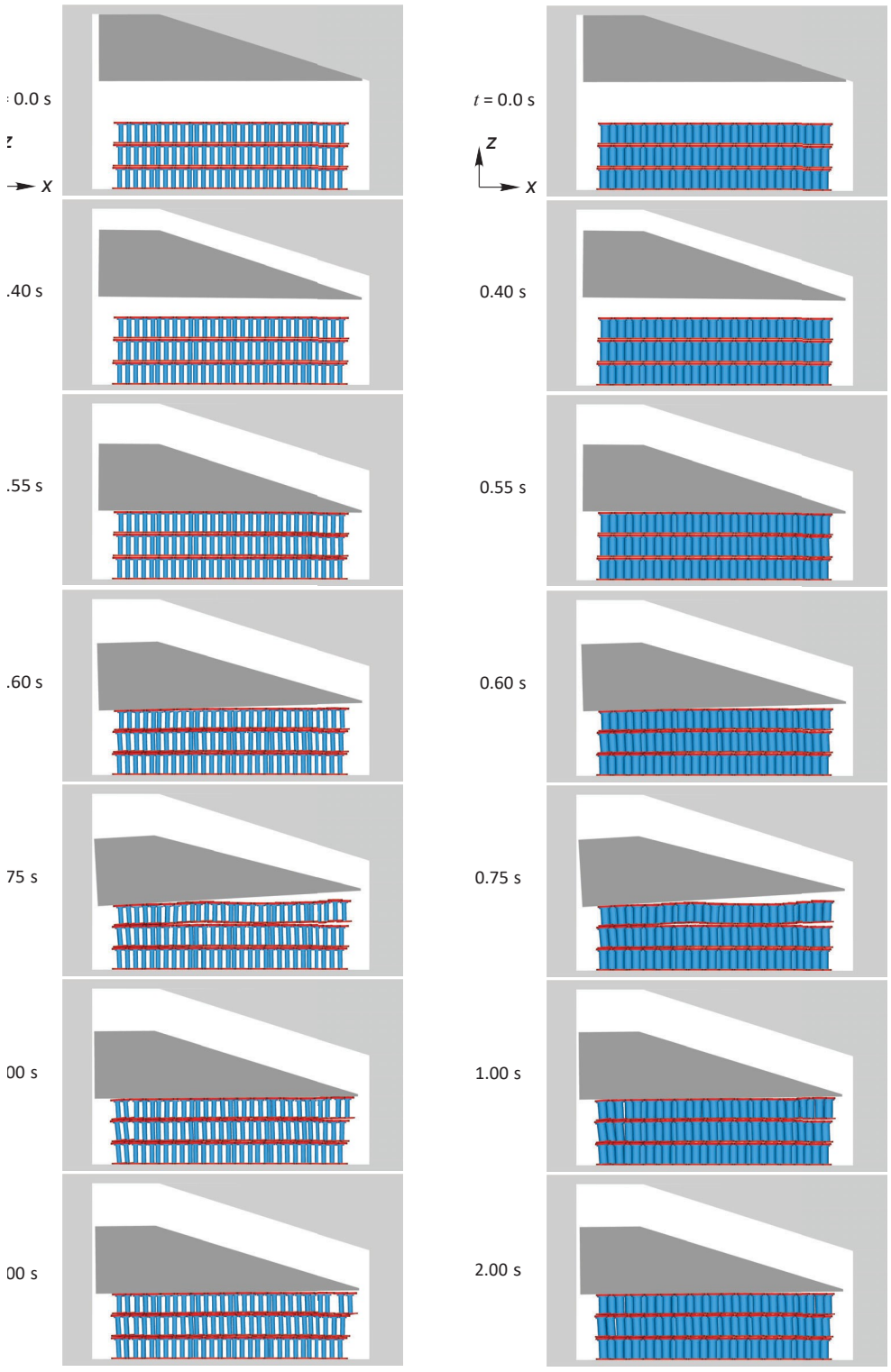

(a) 6-inch Standard POC (b) 12-inch Standard POC

Fig. 12. Negligible deformation and disruption of containers after large trapezoidal-shaped block falls onto room filled with POCs emplaced in a hexagonal array, where blue is flanged inner pipe, and red is top and bottom plywood spacer; fiberboard impact absorber and outer 55-gallon overpack drums are present but removed in visualization.[15, Fig. 19;23, Fig. 3-1]

IV. ANALYSIS OF ROOM CLOSURE FROM SALT CREEP

Room closure from salt creep that compacts the containers was the second modeled repository condition.

IV.A. Compaction Analysis of POCs in 2009

For CRA-2009, supplemental analysis was conducted on the compaction of POCs.[54] A room of POCs were modeled as a homogeneous, isotropic waste block, rather than as 6804 individual containers. The compaction properties of a homogeneous block (e.g., Young's modulus) was assigned the engineering properties of an individual POC, as estimated by hydrostatic, uniaxial tests.[76;77]

For the stiff POC, however, this assumption is not necessarily reasonable because individual POCs are not structurally connected in the 7-pack ensemble and will buckle and tip over. Hence, the POC ensemble in 2009 was modeled much stiffer than likely. Specifically, the final room porosity for a POC filled room with no gas generation was fairly large at 0.612,[g] based on analysis with SANTOS,[78] (versus 0.243 for standard waste drums discussed in §VII).[54, Figure 36] Yet, an alternative approach awaited more advanced computational capabilities now available.[23]

Furthermore, the concern for criticality with POCs is not necessarily that the waste inside the pipes is compacted to a critical concentration (since each POC can only contain 200 FGE) but that the space between POCs decreases such that neutrons interact as a critical array.

IV.B. Conceptual Model for High-Fidelity Salt Creep Simulations

IV.B.1 Salt Creep Constitutive Model

The driving force for room closure is shear stresses in the salt surrounding a disposal room. Salt creeps in the presence of shear stress, and a large void space within a geologic salt formation, such as a room, causes large shear stresses. As the salt creeps into the room, it gradually compacts the containers. Salt creep is a microphysical process due to dislocation glide and pressure solution.[79]

In the current high-fidelity simulations, salt creep is modeled with an updated Munson-Dawson constitutive model that matched vertical closure rates measured at WIPP when using laboratory measured salt properties without adjusting model parameters.[79]

The analysis used the Sierra/Solid Mechanics finite-element code system.[80] The simulations used explicit dynamic numerical solution where the salt visco-plastic strain rate was scaled (sped up). The scale factor was small initially and then gradually increased by several orders of magnitude over the course of the simulation.[23]

IV.B.2. Geomechanical Model

A geomechanical model that includes individual POCs was constructed to predict a representative final configuration of POCs after room closure in the plastic halite. Modeling individual POCs during room closure is computationally difficult and only became reasonable in the last 10 years.[23]

Room closure is a macroscopic geomechanical process that depends on room size, room shape, room contents (i.e., payload containers), and salt stratigraphy (i.e., arrangement of halite, anhydrite, polyhalite, and clay layers—Fig. 9).[79]

The geomechanical analysis models a 2.15-m slice of a room (*y*-direction) in the lower repository horizon that is 10.06-m wide (*x*-direction) and 3.96-m high (*z*-direction), like the roof fall analysis. In particular, the model represents a segment in Room 4 (middle of a panel of 7 rooms) halfway down the 91.4-m room axis (Fig. 6) where the ratio of vertical to horizontal compaction is likely the greatest. In comparison, the most vertical closure is likely to occur at the intersection of straight room segment with an end drift. The location of the greatest horizontal closure might also be of interest, but the location cannot be discerned without detailed three-dimensional studies.

The clay interbeds near the repository are included in the model because slippage in the clay influences the rate and extent of vertical and horizonal salt movement (Fig. 9). Slippage/sliding along the clay layers was modeled using Coulomb friction. The friction coefficient (μ) was set at 0.5 for the most influential nearby Clay F and Clay G seams.[23;81] No difference exists in the mechanical properties between argillaceous halite and halite and so the geomechanical model does not distinguish between the two materials (Fig. 9).[81]

The closure analysis does not include rockfall. Rockfall would tend to make the room more circular, reduce stresses, and, thereby, decrease the closure rate. Yet, roof fall also enlarges the room, which would have the opposite effect of increasing stresses and increasing the closure rate.[82, Ch 6;83] A reduced creep rate caused by the room becoming more circular is thought to dominate, but numerical difficulties thwarted efforts to demonstrate the competing phenomena by combining roof fall and gradual compaction.[23]

Four POC components (internal stainless-steel pipe, its plywood stabilizer on the top and bottom, the fiberboard impact absorber, and outer 55-gallon carbon-steel drum shell with 0.57-m inner diameter—Fig. 4) are

[g] The initial room porosity was 0.843 for room filled with POCs versus initial porosity of 0.848 for room filled with standard drums (as discussed in §VII).[54, p. 93] The stainless steel inner pipe and fiberboard impact absorber do not substantially increase or decrease the initial drum porosity and, therefore, the initial room porosity is almost the same as with standard waste drums.

discretely modeled as individual elastic-plastic-failure material.[23]

With a disposal room filled with 7-pack hexagon bundles of POCs, a 2.15-m slice in a disposal room cuts 36 POCs in half in 3 tiers (12 POCs in one tier). Mirror boundary conditions are used on either side of the slice to represent infinitely long room.[h] Half POCs cannot buckle in the direction of the mirror boundary and cause numerical difficulties with shell elements, as considered here for the pipes in the POCs. Hence, the 36 one-half POCs are eliminated in the analysis; such that 153 discrete whole POCs are modeled (Fig. 13). Reducing the material in the room permits slightly more room compaction.[81]

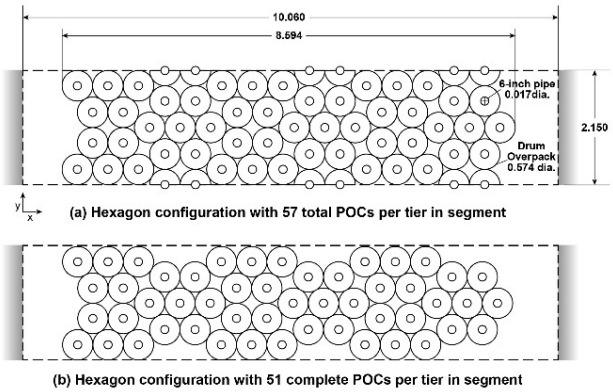

Fig. 13. Slice of WIPP disposal room filled with POCs (a) ideal hexagon array of 57 POCs in one tier at emplacement (171 POCs in 3 tiers—1.85 kg $^{239}Pu/m^2$), (b) deleted 12 half POCs in a tier (153 POCs in 3 tiers—1.66 kg $^{239}Pu/m^2$) in geomechanical model.

Besides removing the 36 half POCs, additional conservative assumptions are used that promote more compaction than would likely be observed:[23] (1) gas pressure from cellulose degradation and metal corrosion, which would normally arrest compaction, is not included;[22] and (2) finite elements of container constituents are deleted from the simulation once they become severely distorted or fractured (e.g., plywood spacers quickly splinter and, thus, not many plywood elements remain at 1000 years).

Like the roof fall analysis,[23] (1) polypropylene bags of MgO are omitted to reduce the volume filling the disposal room by an average of ~3.5% (Table VI); (2) plywood failure strength is reduced 80% to allow greater inner pipe movement; (3) the stainless-steel pipes are empty; thus, structural stiffening from TRU waste is omitted; and (4) the minimum yield strengths of stainless and carbon steel are used.

These conservatisms likely compensate for any additional compaction that could occur because of (1) POC corrosion in the first 1000 years, which would be small without much brine inundation, and (2) continued weakening of stainless steel at the very slow creep strain rates after its initial failure.

A grid convergence study has not been conducted on the container mesh. However, the influence of too coarse a finite mesh, which could reduce compaction somewhat, is expected to be minor, especially, for 6-inch POCs since most 6-inch POCs quickly topple on their sides, as described in the next section.

More importantly, the finite element mesh is like recent models with an empty room. The results of the empty room have (a) compared favorably with international codes, and (b) been verified in grid convergence studies.[82] Furthermore, the empty room closure model was validated against horizontal and vertical closure rate measurements.[79] These measurements were collected from three different empty rooms at the WIPP, over 5.7 years after room excavation.

IV.D. POC Deformed Irregular Array

Shortly after the room ceiling contacts the POC drums (~40 years after closure for drums in the room center and ~70 years for drums near the room walls) some of the POC drums begin to buckle (~100 years for drums in the room center in the middle tier), when modeled as elastic-plastic-failure material (Fig. 14). Buckling allows the drums to slide past each other (especially the POC pipe within the drums).[23] Many other POC drums topple over. Once the drums topple or buckle, they offer little resistance to vertical room closure (i.e., drums represented by a discrete, unconnected ensemble compress far more than drums represented by a single, isotropic material). By 200 years, a substantial number of POCs have toppled or buckled.

The behavior differs between the 12-inch and 6-inch POCs. The 12-inch POC shell buckle but remain mostly upright by 200 years while the 6-inch POCs undergo column buckling and many tip over in the room center by 200 years (Fig. 14). The 6-inch and 12-inch POCs remain in 3 tiers at the edge of the disposal room at 200 years.

More revealing perspectives of POC compaction are the plan and side views of POC centerlines at 1000 years. The 12-in POCs are still mostly upright in two layers in the room center. In contrast, many 6-in POCs are on their side and a single layer has formed in the room center by 1000 years (Fig. 15).

POCs are not noticeably clumped or bunched together down the axis of the room (i.e., *y*-direction). The final coordinate positions of the centroids of each POC are used in subsequent criticality calculations in which

[h] A mirror boundary condition implements a plane strain solution. A mirror boundary is slightly stiffer than a periodic boundary. Although a periodic boundary may converge faster with increasing room length, a periodic boundary is difficult to implement.

spheres of fissile material, bound by the original POC diameter, are placed at the POC centroid.[i]

[i] The POC analysis here used the centroid rather than the center of the centerline of the POC axis. The centroid may be displaced off the POC centerline when the POC buckles. CCO analysis, described in a companion report, used the centerline center to avoid unnecessary confusion because the difference is usually small (Fig. 15).[9]

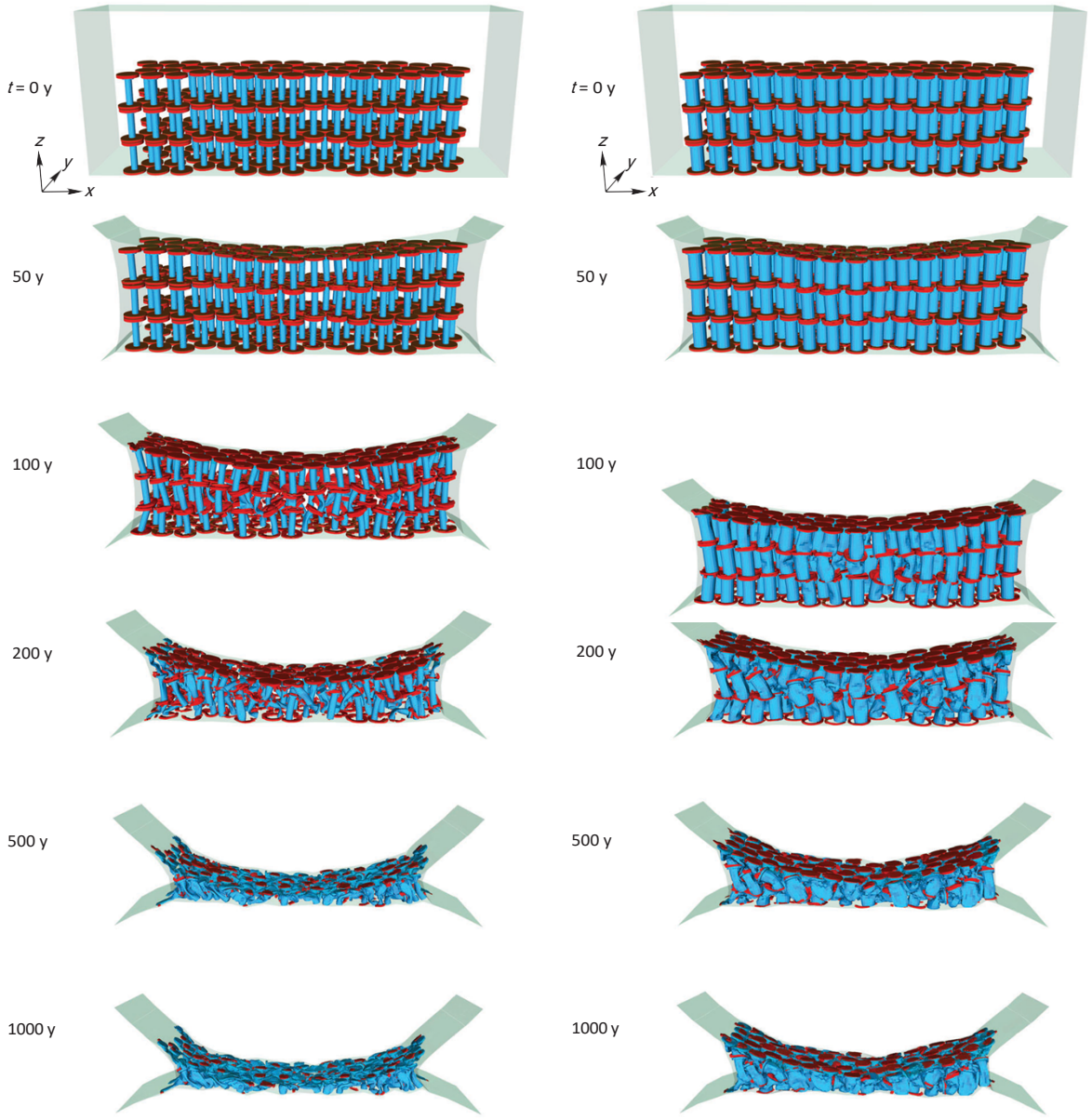

(a) 6-inch Standard POC (b) 12-inch Standard POC

Fig. 14. Deformed inner pipes of standard POCs emplaced as hexagonal array in representative WIPP disposal room closed by salt creep; red elements represent plywood spacers, which stabilize the pipe, but many disappear because they are deleted when they splinter and fail; the outer drum, fiberboard impact absorber, and bedded salt stratigraphy are included in analysis but removed in visualization.[15, Fig. 20;23, Fig. 3-2]

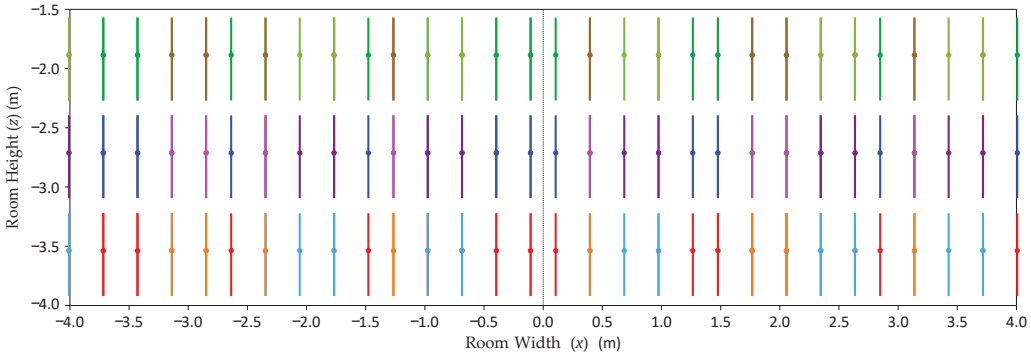

(a) POC hexagonal array side view at 0 years (1 m gap to wall omitted)[70, Fig. 7a]

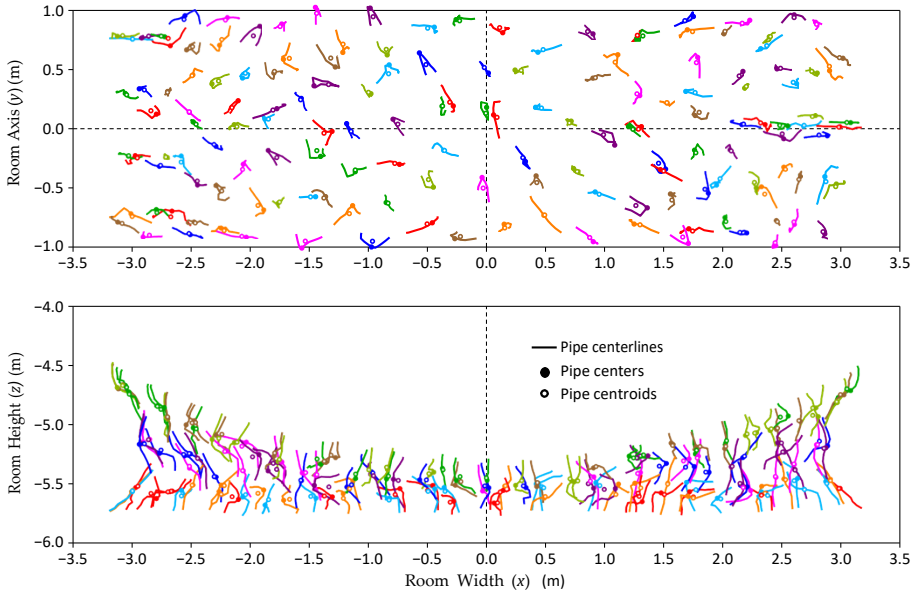

(b) 12-inch POC plan and side view[23, App. B;70, Fig. 37a]

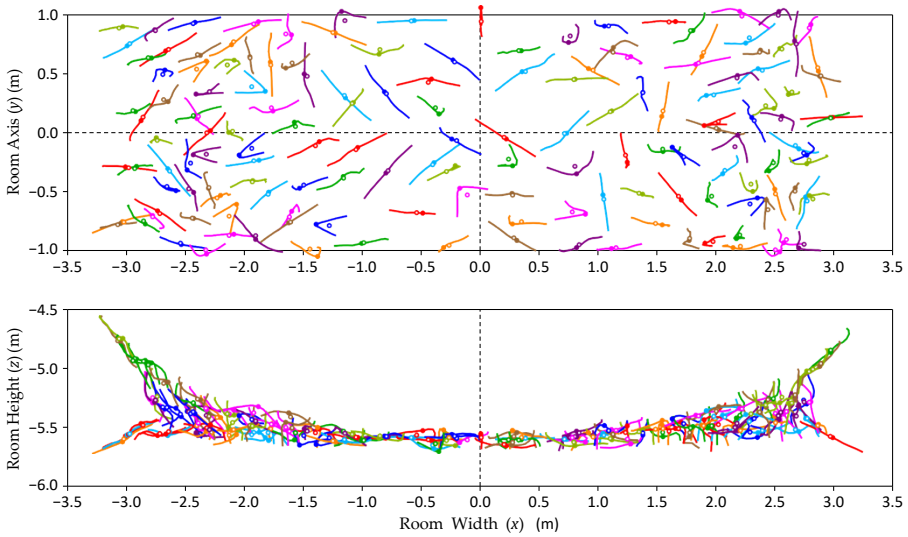

(c) 6-inch POC plan and side view[23, App. B;70, Fig. 35a]

Fig. 15. Deformed centerlines, centers, and centroids of inner pipes of standard POC at 1000 y with friction coefficient of 0.5 for Clay F and Clay G layers.

IV.E. Closure Measure of Deformed Array

Three summary measures of the deformed 12-inch and 6-inch POC arrays are considered to quantitatively compare the extent of clustering: (1) room closure at the disposal room mid-height and mid-width (described here), (2) distance to nearest neighbor POCs (§V.F), and (3) the distribution of POC concentration within the room (§V.G).

Whether a room is empty or filled, most closure occurs vertically. An empty room is mostly vertically closed at mid width by 180 years, and completely closed by 400 years.[82] For a room full of POCs, most closure occurs by 500 years, but continues to close up to 1000 years. For 6-inch POCs, the vertical compaction at the room mid width is 95.3% of the original 3.96 m at 1000 years (i.e., 19 cm remaining—Fig. 16). For 12-inch POCs, the vertical compaction of 88.1% at 1000 years is noticeably less (i.e., 48 cm remaining—Fig. 16).

The horizontal closure at mid-height of an empty room is reduced to 42.7% of its original 10.06 m by 400 years.[23;82] For 12-inch POCs, the horizontal closure at the room center is 40.8% at 1000 years (Fig. 16). For 6-inch POCs, the horizontal closure at mid-height is 43.9% at 1000 years. An empty room has slightly less horizontal closure than a room filled with 6-inch POCs because the vertical closure is so rapid that it pinches off horizontal closure.

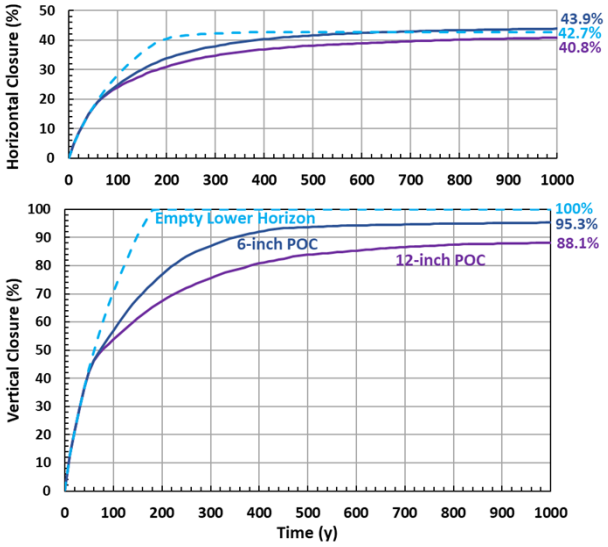

Fig. 16. Horizontal and vertical closure at mid-height and mid-width of WIPP disposal room filled with 6-inch and 12-inch POCs in lower repository horizon (rooms in Panels 1, 2, 7, 8, and 10).[15, Fig. 21;23;82]

IV.F. Nearest Neighbor Measure of Deformed Array

A second summary measure of room closure is the distance to nearest neighbors. At 1000 years, the minimum distance between nearest neighbor centroids for 12-inch POCs is 23.3 cm, which occurs in the center of the room; the maximum distance is 44.5 cm (Fig. 17).[23, Table 3-2] The mean and median distance is 31.8 cm.

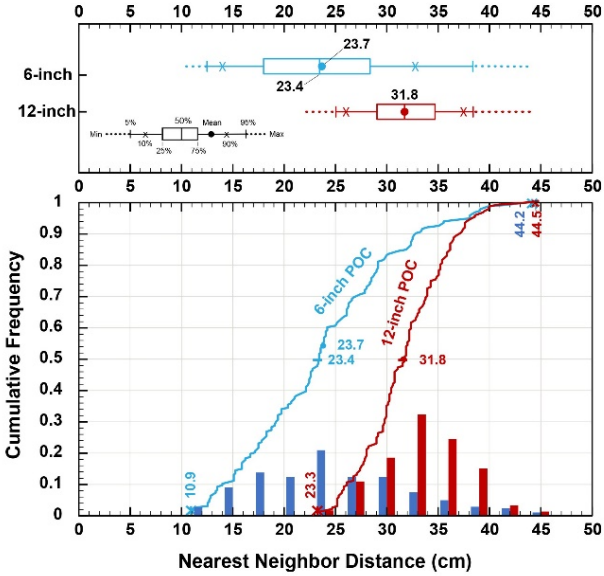

Fig. 17. Distribution of distance between POC centroids at 1000 years based on nearest neighbor: 12-inch POC with 31.8-cm average/23.3-cm minimum; and 6-inch POC with 23.7-cm average/10.9-cm minimum.[23]

A room with 6-inch POCs has a somewhat wider distribution with a mean and median distance of 23.7 and 23.4, respectively; the minimum is 10.9 cm, which occurs near the room center; the maximum is 44.2 cm. Hence, by modeling 153 discrete POCs, the calculation produces a wide variety of deformed spacing between POCs.

IV.G. POC Concentration Measure of Deformed Array

A third summary measure of the room considered is the uniformly weighted POC concentration ($c_{uniform}$), which is also the fissile concentration at 200 FGE ^{239}Pu per POC, defined as

$$c_{uniform} = n_{POC} / V_{sphere} \quad (2)$$

where n_{POC} is the number of POC in a sphere volume V_{sphere} calculated as $4\pi(r_{sphere})^3/3$ based on a specified defined sphere radius r_{sphere}. Here, we evaluate the concentration in a 75 cm radius sphere about each centroid (which corresponds to almost 4 orders of

magnitude reduction in neutron flux through salt—see §VII.C). The initial concentration is between 2.26 and 3.96 POC/m^3 (Fig. 18). The lower value is for 6-inch and 12-inch POCs near the salt wall; the upper value is for POCs in the center of the array.

For the 12-inch POC, the mean concentration after deformation is 9.6 POC/m^3—1.9 kg Pu/m^3 and the maximum concentration is 13 POC/m^3—2.6 kg Pu/m^3 (Fig. 18) The 6-inch POC has a fairly uniform distribution with a higher concentration than 12-inch POC (mean of 11.2 POC/m^3—2.2 kg Pu/m^3 and maximum of 17 POC/m^3 –3.4 kg Pu/m^3), which is consistent with the smaller distance to the first nearest neighbor (mean of 23.7 cm for 6-inch POC versus 31.8 cm for 12-inch POC).

The highest POC concentrations are near the collapsed room wall (between 20% and 50% of the distance to the room center—Fig. 19) unlike the situation for nearest neighbors, which can occur anywhere in the disposal room. For example, the largest nearest neighbor occurs near the room center for the 12-inch POC and near the room wall for the 6-inch POC.

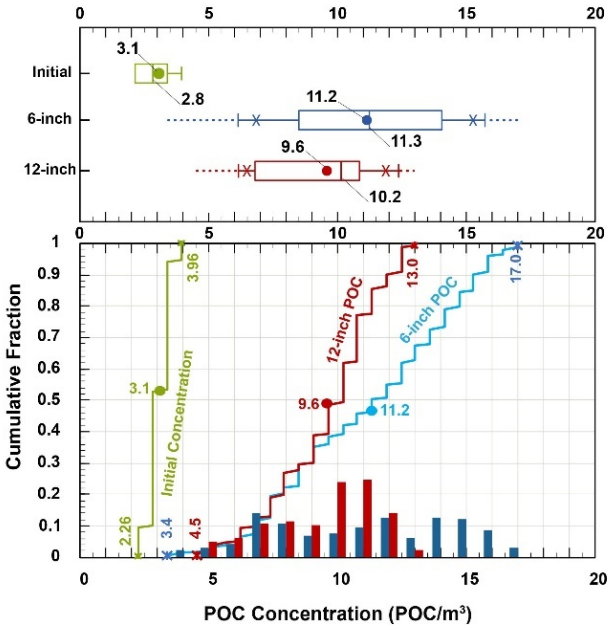

Fig. 18. Distribution of POC concentration in 0.75 m sphere about each centroid at 1000 years.

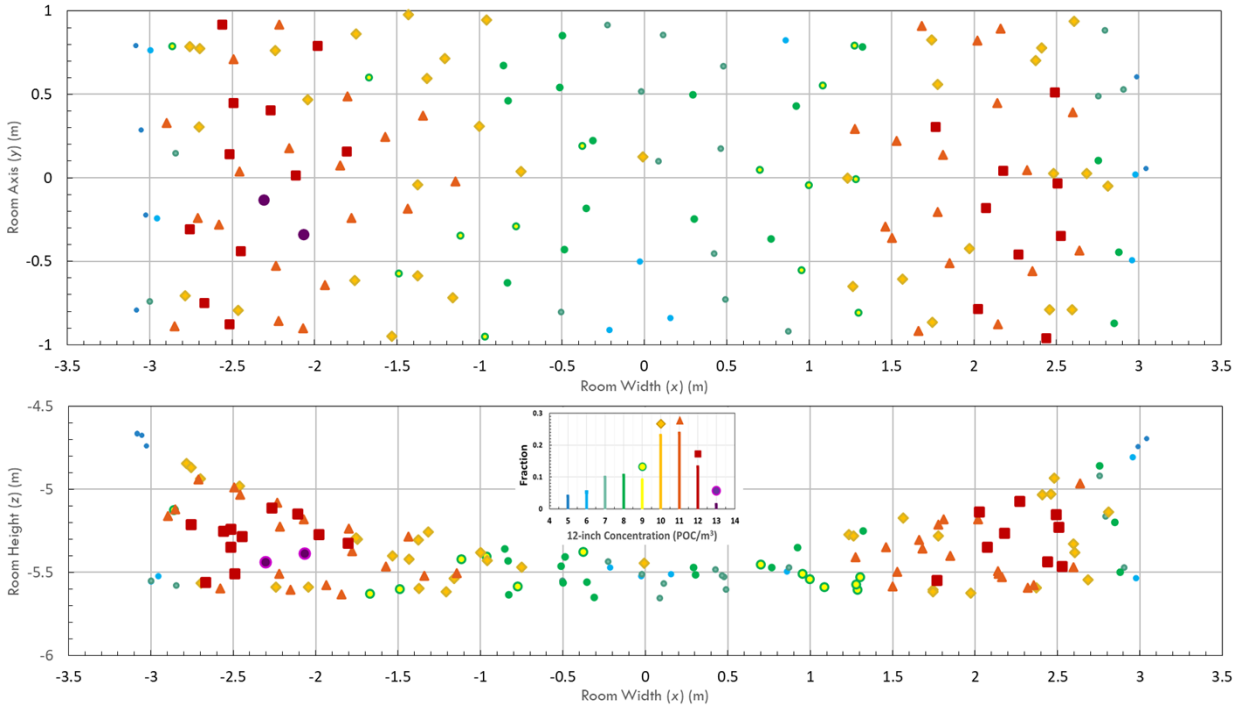

(a) 12-inch POC plan and side view[70, Fig. 37b]

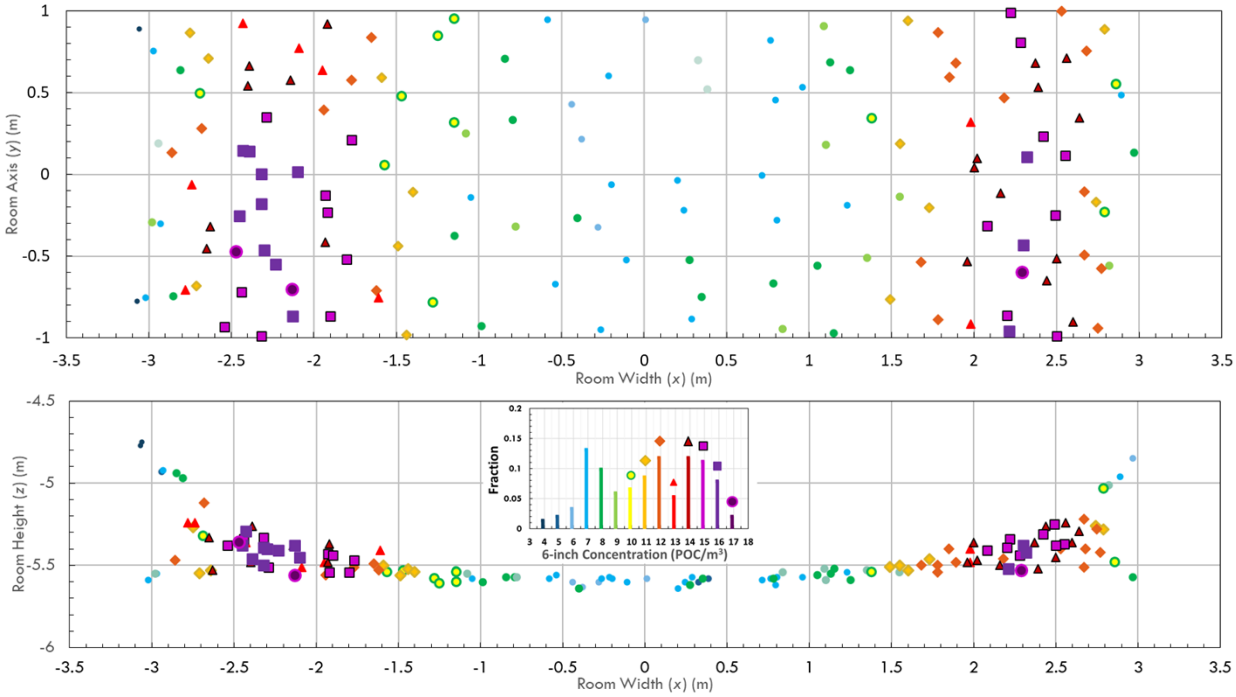

(b) 6-inch POC plan and side view[70, Fig. 35b]

Fig. 19. Number of centroids in 0.75-m radial sphere at each of 153 POC locations in 2.15-m disposal room segment in lower repository horizon.

V. CRITICALITY EVALUATION OF POC IRREGULAR ARRAY

V.A. Computational Tool and Upper Subcriticality Limit

To evaluate the post-closure criticality potential of the compacted rooms,[84] a series of models were developed with MCNP™ (Monte Carlo N-particle code for solving Neutron and Photon transport equations),[85] Version 6.2 using the 238 group Evaluated Nuclear Data File/B Version 7.1 (ENDF/B-VII.1) criticality library of tabulated cross-sections, which is provided in the standard release of MCNP.

The upper subcriticality limit (USL) at which a fissile configuration is considered critical is derived from the bias and uncertainties associated with MCNP, the underlying nuclear data, and the modeling fidelity.[j] For a geologic disposal system, however, phenomenological modeling, such as geomechanical modeling of salt creep, is necessary to predict plausible configurations. The factors that influence the uncertainty in plausible configurations, such as variation in initial conditions of waste and variation in host rock characteristics (e.g., porosity, saturation, and host rock composition) cause larger changes in the minimum masses and concentrations than the small calculational biases and uncertainties in neutron/photon transport for criticality evaluation (i.e., the uncertainty in specifying the physical state of POCs after 1000 or more years, using Sierra/Solid Mechanics finite-element code system,[80] is similar or larger than the neutron calculation uncertainty and bias in codes like MCNP, where the average uncertainty in the MCNP analysis ($\overline{\sigma}^{MCNP}$) of the multiplication factor for a finite system (k_{eff}) is ~0.0006.[84, p. xiii] Furthermore, EPA envisions an approach based on reasonable expectation using mean or representative values. Hence, for post-closure criticality evaluation at WIPP, USL is set at unity and the $2\overline{\sigma}^{MCNP}$ offset for k_{eff} is omitted. Thus, a postulated assembly of fissile material in a geologic setting after WIPP closure is subcritical when the criticality index $k_{eff} < 1.0$.

The analysis here is to ensure criticality has a low probability of occurring such that it can be excluded from the PA, when humans are absent. The analysis does not relate to nuclear criticality safety during transportation or operations when humans are present.

[j] A fissile system is "critical" when a nuclear chain reaction is sustained, which is expressed by a neutron multiplication factor (k) of unity, where k is conceptually the number of neutrons in one generation divided by the number of neutrons in the prior generation. Traditionally, k_{eff} denotes a multiplication factor for a system of finite extent, and k_∞ denotes a homogenous system of infinite extent.[86, pp. 75-84]

V.B. POC Conceptual Model for Criticality Evaluation

For a finite heterogeneous system, criticality depends upon (1) type, mass, and form of fissile material; (2) shape including individual and array configuration of fissile regions; (3) material mixed with the fissile material and its overall concentration; and (4) nearby material and its concentration outside the fissile array.

V.B.1. Plutonium Waste Form and Mass

Plutonium was modeled as plutonium dioxide (PuO_2 with ρ_g = 11 460 kg/m^3 and 88% of density as Pu^{IV}), rather than modeled as metallic Pu or Pu with water of hydration or hydroxyl groups (i.e., $PuO_2(OH)_2 \cdot H_2O$ or $Pu(OH)_4$). For highly enriched ^{239}Pu, the mineral form only influences criticality limits when the mixture is severely under moderated (Fig. 20).[13]

The POC plutonium content is set at the administrative limit of 200 FGE ^{239}Pu (Table IV) and modeled as 100% ^{239}Pu. Although other fissile isotopes possibly mixed with ^{239}Pu influence criticality, we bound the isotopic influence including changes with decay over the 10 000 y-regulatory period by adopting the concept of FGE (Table I).

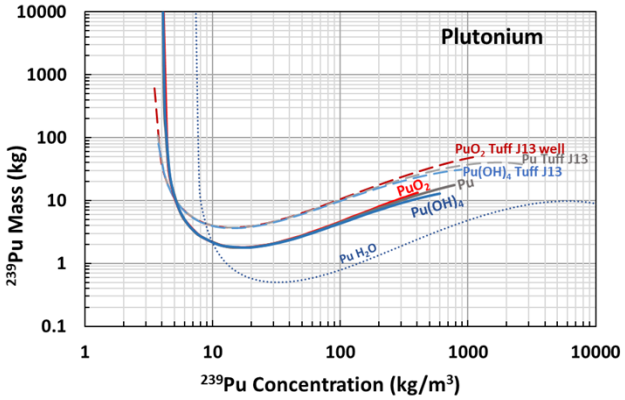

Fig. 20. Mineral form of highly enriched Pu only influences criticality limits for sphere when mixture is severely under moderated.[12, Fig. 7;13, Fig. 8]

V.B.2. Array Configuration and Fissile Shape

The fissile waste and any mixed material (Region 1) are configured as an irregular array in a sea of reflecting material (Region 2) confined by a tightly fitting box with dimensions defined by the maximum extent of the spheres. Salt is placed in an outer Region 3 (beyond the Region 2 reflector box) as a 10-m outer layer (Fig. 21).[84]

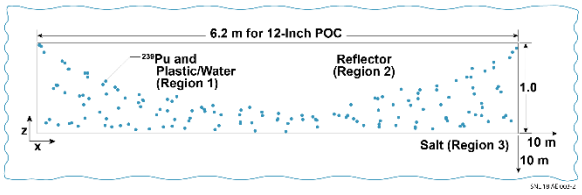

Fig. 21. Three material regions of MCNP criticality model, with dimensions of Region 2 defined by maximum extent of the centroid coordinates of the POC inner pipe.

The Pu configuration in Region 1 is spherical to avoid making assumptions as to the distribution of Pu in each POC and the compaction of that material within the POC from room closure. The ^{239}Pu density of a sphere with the inner diameter of a 12-inch POC (31.4-cm) is 12 kg/m^3; the ^{239}Pu density in a 6-inch sphere (15.8 cm) is 98 kg/m^3 (factor of 8 larger than for the 12-inch sphere). The influence of room closure is primarily on the disrupted configuration and decreased spacing between the array of spheres.

V.B.3. Hydrogenous Material Mixed with Fissile Material

The hydrologic regime in the spherical Region 1 evolves from moderation with water/polyethylene to moderation with Castile brine/polyethylene in the cases reported here (Table VII).[84] Polyethylene (CH_2) lines the POC overpack (Fig. 4) and may be used to bag Pu or Pu-contaminated articles in the POC.

A POC was assumed to contain sufficient fluid and polyethylene in a volume ratio of 3:1 (where the plastic volume cannot be replaced with brine) for the Pu waste form to be nearly optimally moderated with hydrogen to avoid making specific assumptions as to the pathway to criticality and the mineral form of Pu. The optimum moderation was evaluated for each case analyzed.[84]

A Pu-polyethylene mixture has reduced minimum mass compared to a Pu-water mixture. As an example, for a sphere of ^{239}Pu mixed with water and polyethylene at ratio of 3:1, the critical limits decrease from 0.51 to 0.47 kg (at 34 kg/m^3 concentration) and the asymptotic concentration increases from 7.3 to 7.7 kg/m^3 (Fig. 22).

A 200-g Pu sphere at 34 kg/m^3 optimum concentration corresponds to 11.2-cm radius, which is <15.6-cm inner radius of 12-inch POC but >0.077-cm inner radius of a 6-inch POC (Fig. 23); thus, a 0.2 kg sphere of ^{239}Pu that fits inside a 6-inch pipe cannot be optimally moderated.

Hence, the critical potential is reported for (a) an unconstrained diameter sphere, (b) a sphere constrained by the 6-inch pipe inner diameter and, thus, not optimally moderated, and (c) a cylinder constrained by the 6-inch pipe inner diameter. The latter limit is reported since a cylindrical shape with radius limited by the 6-inch pipe may be somewhat more reactive than a sphere constrained by the 6-inch radius since the cylinder shape can accommodate more moderating hydrogen.

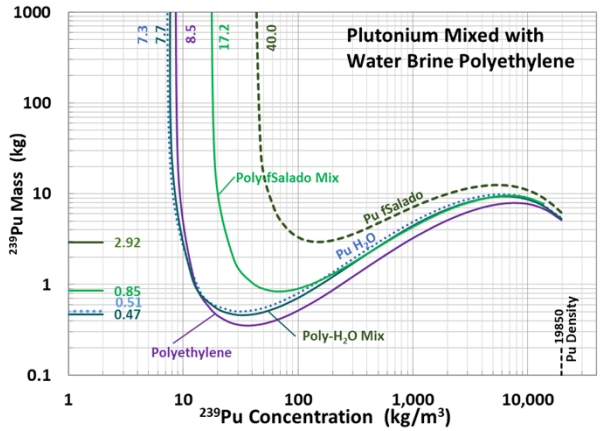

Fig. 22. Critical limits for ^{239}Pu sphere mixed with water, Salado brine, polyethylene, and volume mixture of 25% polyethylene, 74% fluid (water or Salado brine), and 1% beryllium as used in detailed ORNL MCNP criticality model.[12, Fig. 10]

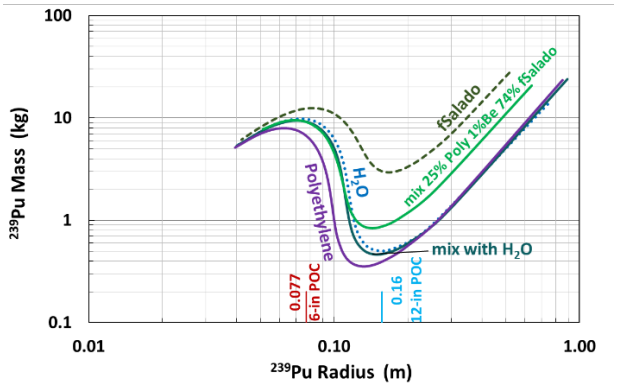

Fig. 23. Critical ^{239}Pu sphere radius in water, Salado brine, polyethylene, and volume mixture of 25% polyethylene, 74% fluid (water or Salado brine), and 1% beryllium compared to radius of 6-inch and 12-inch POCs.[12, Fig. 10]

V.B.4. Material in Reflector Box Surrounding Fissile Region

The hydrologic regime of the Region 2 reflector sea surrounding the fissile Region 1 changes to reflect the disposal room evolution: (1) salt creep compaction of containers without brine influx (which permits maximum compaction), (2) influx of sufficient brine to allow cellulose degradation and to partially saturate pores, and (3) brine inundation to complete cellulose degradation.

Iron is always modeled as rust hematite (Fe_2O_3 with Fe^{+3}) even though it is present in the stainless-steel pipes and carbon-steel drums primarily as metallic iron (Fe^0) in the first 1000 years. The oxidation state of Fe is

immaterial. The mass of stainless steel in the pipe of the 12-inch POC is 57.3 kg (assuming the 304 stainless steel density is 7940 kg/m^3 and the volume is 7215 cm^3).[84]

Beryllium (Be) is a possible element of some TRU waste and potentially important because its decay contributes neutrons. Be was set at 1 wt. % (i.e., 1.02 kg in the 12-inch POC and 0.30 kg in the 6-inch POC). Most POCs do not have any Be and only 34 twelve-inch POCs in Panel 7 from Los Alamos National Laboratories (< 0.13% by volume) report Be >1 wt. %. Although included for completeness, sensitivity studies showed no influence whether mixed in the fissile material sphere (Region 1) or in the reflector sea around the fissile sphere (Region 2).

The 25.2 kg of fiberboard initially present in a 12-inch POC reduces the neutron coupling between POC until it microbially degrades with brine influx. In the criticality evaluation, fiberboard is modeled as cellulose ($C_6H_{10}O_5$) with a density of 224 kg/m^3.[84]

MgO with its large neutron scattering cross-section, acts as a good neutron reflector. MgO is emplaced above the containers but likely sifts down the containers sides when room closure bursts the polypropylene bags. The MgO readily flows around and into the containers once brine inundates the disposal room; thus, MgO is mixed homogeneously with other material in the reflector box in the second (transition from dry) and third (final) hydrologic regimes of the repository.

Salt is present as a neutron absorber/reflector[k] in the Region 2 reflector box in the last hydrologic regime, in addition to the salt in Region 3.[84] The ratio of MgO volume to salt volume around the containers is set at 1:1 in the studies reported here, which bounds the MgO placed in rooms in the first few panels (Table VI).[84]

The volume of the reflector box at 1000 years when modeling 153 12-inch POCs is ~13.3 m^3 (i.e., 6.2-m length, 1.0-m height, and 2.15-m width— Fig. 19a, Fig. 21) and ~12.4 m^3 when modeling 6-inch POCs (i.e., 6.05-m length, 0.95-m height, and 2.15-m model width—Fig. 19b). For MgO with a grain density of 3600 kg/m^3 and final total room Eulerian porosity of 0.261 (§VI.A.2), the MgO mass in ½ of the reflector box for 12-inch POCs is 35.4 t (or 109 kg per POC stack).

In comparison, Panel 1 with the 3.2 t Pu residues in ~17 000 POCs had ~ 13.9 t MgO in bags on every 7-pack of POCs (~7.3 bags with 1905 kg of MgO per bag in the modeled room segment). Hence, the model has a factor of ~1.6 more MgO than in a room in Panel 1 and a factor of ~3.2 more MgO than in a future room of 12-inch POCs.

[k] The Cl of NaCl absorbs neutrons (especially when brine is present) but the crystalline salt also acts as a reflector.

V.C. Criticality Evaluation of Closed Room without Brine

V.C.1. Waste Conditions Inside POC Pipe

The first hydrologic regime assumes mostly dry conditions outside the POC to allow maximum compaction of the room with little gas generation. The hydrogenous moderator inside the POC is a 3:1 mixture of water to polyethylene inside the POC inner pipe.

V.C.2. Conditions Outside POC Pipe

Conditions envisioned outside the POCs up to 1000 years include (1) iron between spheres (e.g., 57.2 kg of iron in 12-inch stainless steel pipe) but modeled as iron oxide (Fe_2O_3); (2) no brine between POC spheres; (3) no salt between POC spheres because the salt may not have had time to completely encapsulate the waste; (4) no MgO between POC spheres; and (5) >60% of fiberboard impact absorber remaining.

The 60% of fiberboard remaining in the POC is based on the minimum amount of cellulose that remains in the entire repository at 1000 years in the CRA-2019 repository exposure model when accounting for uncertainty in parameters and conditions for the undisturbed scenario (Fig. 24). Because this value will change with each PA, using an extreme minimum rather than the mean ensures that the results will not be sensitive to each periodic PA.

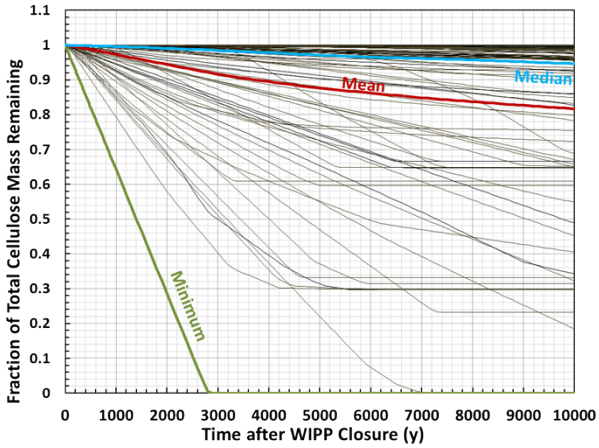

Fig. 24. Cellulose mass remaining throughout repository for undisturbed scenario in 100 simulations of Replicate 2 (mean and median displayed is based on all 3 replicates of CRA-2019).[15, Fig. 24]

V.C.3. Results for Closed Room without Brine

With >60% of the initial fiberboard present in the first 1000 years, a room full of 6-inch or 12-inch POCs is subcritical. A room with 6-inch POCs has higher k_{eff} consistent with the higher geometric concentration (11.3 POCs/m^3—Fig. 18) (i.e., k_{eff} < 0.961 for 6-inch POC and <0.913 for 12-inch POC—Fig. 25).

V.C.4. Sensitivity Cases

Three cases were also run to examine the sensitivity of k_{eff} to type and amount of material between POC when dry. The first sensitivity case included 100% of the initial fiberboard to examine the influence of the conservative assumption on k_{eff} (i.e., the maximum rate of microbial degradation occurs when brine is readily available, which is inconsistent with the assumption of dry conditions and little microbial gas generation in the first 1000 years to allow for the maximum compaction). The influence was small but differed for the 6-inch and 12-inch POC. For the 6-inch POC, more fiberboard increased the maximum k_{eff} by 1% (Δk_{eff} of 0.010 from 0.961 to 0.971); for the 12-inch POC, more fiberboard decreased the maximum k_{eff} by 2% (Δk_{eff} of 0.02 from 0.913 to 0.893 (Fig. 25). The influence of reflector material changes as the pitch between spheres changes.

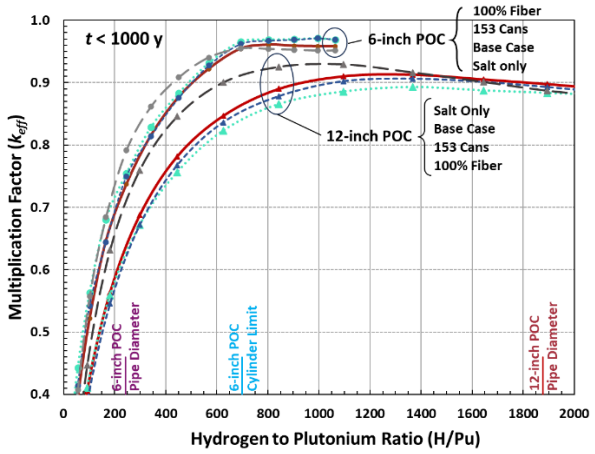

Fig. 25. Multiplication factor for irregular compacted array of 6-inch and 12-inch POCs without brine influx as represented by infinite number or 153 spheres in WIPP room segment with 200 g ^{239}Pu moderated with water/plastics and reflected by salt or iron oxide/fiberboard (where fiberboard set at either 100% or 60% of initial mass).[15, Fig. 25;84, App. G]

V.C.5. Correlation of POC Concentration with Neutron Tallies

The neutron tallies for a selected horizontal slice of the POC irregular array is dominated by several areas on the right side of the WIPP room (Fig. 26). The areas of high neutron tally in the selected slice correspond to areas of high POC concentration (Fig. 19a). For the three most active areas of Fig. 26, one area is at ~12 POC/m^3; the other two areas are at ~11 POC/m^3 in Fig. 19a. The neutron tally plot at one plane suggests that system reactivity of the irregular, non-uniformly compacted POC array is driven by reactivity in a few localized areas exhibiting elevated fissile mass concentrations in comparison to a regular, uniformly compacted POC array that exhibits many areas of high neutron flux distributed over a larger area of the modeled room. A more sensitive measure of container concentration, the relative weighted concentration, is discussed when evaluating CCO arrays in a companion report.[9]

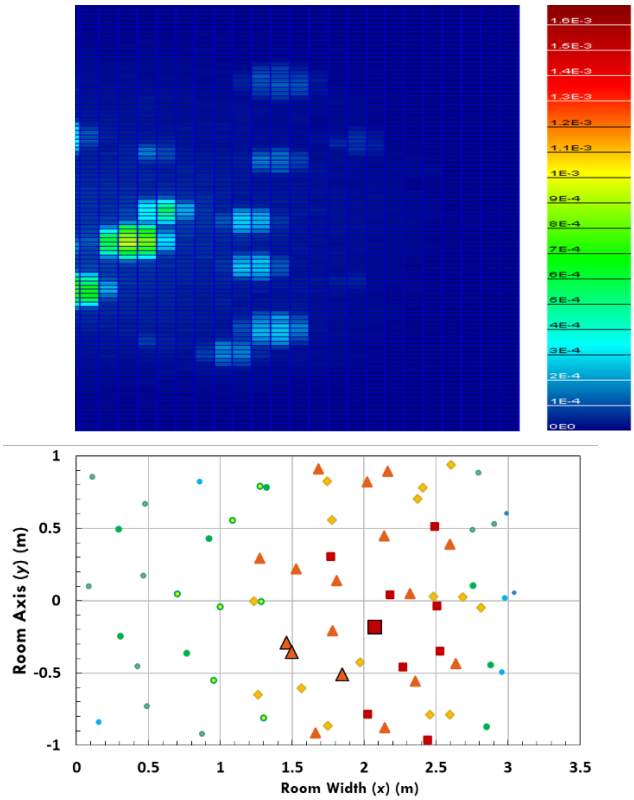

Fig. 26. Neutron tallies at one horizontal slice for 12-inch POC shows k_{eff} dominated by several locations on right side of room that qualitatively correspond to high concentration in Fig. 20a.

V.D. Criticality Evaluation with Partially Degraded Fiberboard and Some Brine

V.D.1. Conditions near POC

At some point, enough brine may enter the disposal rooms (Region 2) such that microbial degradation of the fiberboard occurs along with more corrosion of the POC stainless and carbon steel. Although many combinations of brine and fiberboard can occur during the transition, the second hydrologic regime modeled in the criticality evaluation (at 1000 y < t < 2000 y) assumes that after complete compaction of the POC array occurs influx of enough brine into Region 2 such that (1) 20% of the interstitial space between containers (Region 2 reflector box) is filled with Castile brine but the containers remain sufficiently intact to prevent brine in the fissile Region 1; (2) microbial degradation consumes 60% of the fiberboard; (3) the gas generated from microbial degradation and corrosion reopens the room such that no

salt is in the reflector box; but (4) MgO remains in Region 2 reflector box.

V.D.2. Results with Some Brine Outside POC

While substantial loss of the fiberboard allows more neutron coupling between individual containers, the presence of Cl^{-1} and B^{+3} in the Castile brine dampens room reactivity. The presence of brine in 20% of the interstitial space of Region 2 is sufficient to dominate the behavior of the POC array. For the 6-inch and 12-inch POCs, k_{eff} decreases 6% (Δk_{eff} of 0.059 from 0.961 to 0.902 for 6-inch POC and $\Delta\ k_{eff}$ of 0.058 from 0.913 to 0.855 for 12-inch POC—Fig. 27). The 6% decrease is noticeably greater than the 1 to 2% change in k_{eff} in the sensitivity studies observed prior to brine influx (Fig. 25).

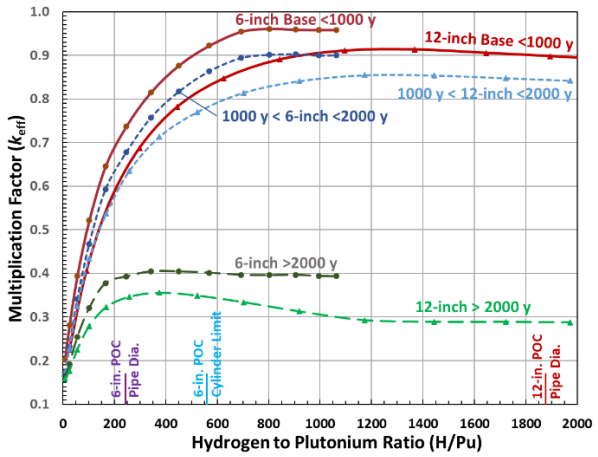

Fig. 27. Multiplication factor for irregular compacted array of 6-inch and 12-inch POCs vary between 0.96 and 0.91, respectively, for conditions without brine, between 0.90 and 0.85 for conditions with some brine between POCs, and between 0.40 and 0.36 for conditions with brine inside POC.[15, Fig. 27;84, App G]

V.E. Criticality Evaluation with Fully Degraded Fiberboard and Brine Inundation

The final hydrologic regime modeled in the criticality evaluation (2000 y< t < 10 000) is where (1) all fiberboard has degraded; (2) POCs have completely degraded but Fe would still be present; (3) Castile brine dominates behavior within $^{239}PuO_2$ waste (Region 1);[1] and (4) salt and MgO is present between the remnants of POCs.

As an alternative, Region 2 could be dry from consumption of brine in metal corrosion, microbial degradation, and MgO hydration. However, brine consumption of water in the metal corrosion, microbial degradation, and MgO hydration leaves Cl^{-1} and B^{+3} behind to arrest neutronic coupling of the fissile material in POCs as the fiberboard is consumed.

For t >2000 y, k_{eff} of the POC room ensemble decreases ~60% from the first hydrologic regime (Fig. 27); specifically, Δk_{eff} of 0.556 from 0.961 to 0.405 for 6-inch POCs and Δk_{eff} of 0.557 from 0.913 to 0.356 for 12-inch POCs.

V.F. Disturbed Conditions

This criticality evaluation of POC compaction from room closure caused by salt creep focuses on the evolution of repository conditions prior to humans unknowingly intruding into WIPP (i.e., undisturbed conditions). Modeling of disturbed conditions caused by inadvertent human intrusion into the repository any time after the first 100 years, as required by EPA in their disposal regulations, does not produce additional conditions conducive to criticality from room closure that are not already captured by an undisturbed scenario with brine influx sufficient to alter all the Fe-based metal and cellulose.

To elaborate, an inadvertent human intrusion by exploratory borehole into the repository relieves gas pressure and induces more room closure and, thus, more closely approximates the first hydrologic regime for undisturbed conditions. If the intrusion intersects a brine reservoir below the repository (see §II.D), the disruption injects more brine into the disposal region than is already present in the undisturbed scenario. The addition of more brine (1) increases the likelihood of the third hydrologic regime where any remaining cellulose and metals are completely degraded, and (2) decreases the likelihood of criticality because of the chloride in the brine (Table VII).

VI. ANALYSIS OF CH AND RH CONTAINERS

VI.A. Compaction of Standard CH Drums

Coupling two-phase flow of brine and gas about the repository with mechanical room closure from salt creep is not computationally feasible in the PA. Instead, the two phenomena are decoupled.[24;63] A porosity response surface is developed to represent the change in porosity of the disposal rooms as a function of the mass of gas present and elapsed time since closure[87,§5.2.3] (i.e., $\phi^{room}(t, f^{gas}(\Gamma^{gas}(t)))$ where the f^{gas} is a gas-generation index function with the gas generation rate $\Gamma^{gas}(t)$ as a parameter.

In the 1996 CCA up through CRA-2019, the porosity surface was abstracted from numerous simulations of the idealized stratigraphy of halite and anhydrites (partially shown in Fig. 9) using the older two-dimensional, finite-element, large-deformation, quasi-static structural mechanics code, SANTOS.[78] Salt

[1] Brine influx and subsequent mobilization, transport, and deposition of fissile material elsewhere in the WIPP disposal system is discussed in a companion report.[10]

creep was modeled using the older Munson-Dawson constitutive model with several parameters adjusted to match room-sized experimental results at WIPP.[69]

Two types of room porosity may be calculated from the same simulations:[63] (1) Lagrangian room porosity ($\phi_{Lgrng}^{room}(\sim)$ —which is the ratio of the calculated void volume at a specified time to the *initial* 3642 m^3 volume of the room); (2) Eulerian room porosity ($\phi_{Elrn}^{room}(\sim)$)—which is the ratio of the calculated void volume to the calculated room volume at a specified time. A Lagrangian room porosity is used in PA calculations because fluid flow simulations do not use a deformed room grid. However, an Eulerian porosity is more meaningful for criticality evaluations and used herein.

VI.A.1. Drum Compaction as Homogeneous Block

When developing porosity surface (i.e., $\phi_{Elrn}^{room}(\sim)$ or $\phi_{Lgrng}^{room}(\sim)$) for the 1996 CCA through CRA-2019, the room of drums and contents are modeled as a single, homogeneous, isotropic volumetric plastic block, rather than as 6804 individual containers,[24] which was seemingly appropriate given the weak crushing strength of a standard drum with uncompacted waste debris.[63] The compressive properties of the isotropic volumetric plastic material were assigned the properties of an individual standard drum from uniaxial and hydrostatic tests.[77]

In the 1996 CCA through CRA-2019, the disposal room compacted from an overall initial room porosity of 0.848 (i.e., $\phi_{initial}^{room} = 0.848$) to a final Eulerian room porosity of 0.243 when the gas generation was zero (i.e., $\phi_{Elrn}^{room}(t > 200y, f^{gas}(0)) = 0.243$, which occurs after ~200 years when there is no metal corrosion of the containers nor microbial degradation of cellulose and plastics promoted by brine influx)

Based on the change in room porosity, the final room density (ρ_f^{room}) increased a factor of 5:[24, Figure 8;54, Figure 34]

$$\rho_f^{room} / \rho_i^{room} = \frac{1-\phi_{Ekrb}^{room}(t > 200y, f^{gas}(0))}{1-\phi_{inital}^{room}} = (1-0.243)/(1-0.848) = 5 \quad (2)$$

Because the entire empty space is removed, the final porosity of the room is about the same as the final porosity of the individual drums. In the 1996 CCA through CRA-2019, initial porosity of an individual drum containing the average components of waste destined for WIPP (Table II) was 0.681 (i.e., $\phi_i^{waste} = 0.681$).[54, p. 19;76;77] Thus, the density increase of the TRU waste was about one-half of the density increase (volume decrease) of the entire room,[m] that is from Eq. (2):

$$\rho_f^{room} / \rho_i^{waste} = \frac{1-\phi_{Ekrb}^{room}(t > 200y, f^{gas}(0))}{1-\phi_i^{waste}} = (1-0.243)/(1-0.681) = 2.4 \quad (3)$$

VI.A.2. Compaction of Individual Standard Drums

As part of an effort to recalculate the porosity surface $\phi_{Lgrng}^{room}(\sim)$ for CRA-2026,[63] the appropriateness of representing standard drums and waste as a single, homogeneous, isotropic, volumetric plastic block was verified with high fidelity simulations using discrete 55-gallon drums, like the approach described previously in §V. The high-fidelity simulations of discrete 55-gallon drums does indeed show behavior that is like a homogeneous block (Fig. 28). In the analysis, the compressive properties of the isotropic plastic materials were based on updated individual uniaxial, triaxial, and hydrostatic tests on simulated waste.[88]

The initial overall room porosity is 0.917 and the final Eulerian room porosity is 0.261 for a hexagonal drum arrangement in disposal rooms in the upper horizon (Fig. 29).[63, p. 47&Fig. 3-15] Hence, the overall density increases a factor of 9. In contrast, the initial drum/waste porosity is 0.825;[63, p. 23] thus, the waste density increases a factor of 4.2 (Eq. (3)), which is about twice the density estimated for the 1996 CCA.

By comparison, 60-MPa super compaction of 55-gallon drums containing debris waste stored at Idaho National Laboratory has a final volume between 15 and 35 gallons, or between a factor decrease of 3.8 and 1.6 of the original volume.[54, p. 23] The factor of 3.8 volume decrease by 60 MPa compaction bounds the factor of 2.5 volume decrease estimated in CRA-1996 and is similar to the factor of 4.2 volume decrease for CRA-2026 estimated from ~14.7 MPa lithostatic pressure at WIPP.

[m] In the criticality screening rationale for the 1996 CCA, the analysis also used the much smaller final Lagrangian room porosity of 0.08 such that the density increased a factor of 6;[1, Fig. 12] that is, $\rho_f^{room} / \rho_i^{room} = (1-\phi_{Lgrng}^{room}(t > 125y, f^{gas}(0)))/(1-\phi_{initial}^{room}) = (1-0.08)/(1-0.848) = 6$. The increase in the density of the drum contents is still ~½ of that of the room (i.e., $\rho_f^{room} / \rho_i^{room} = (1-0.08)/(1-0.681) \approx 3$).

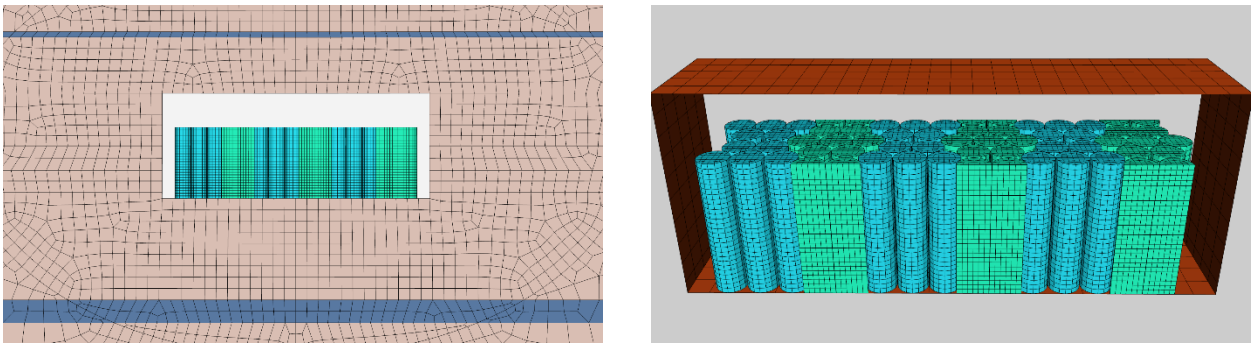

(a) 0 years

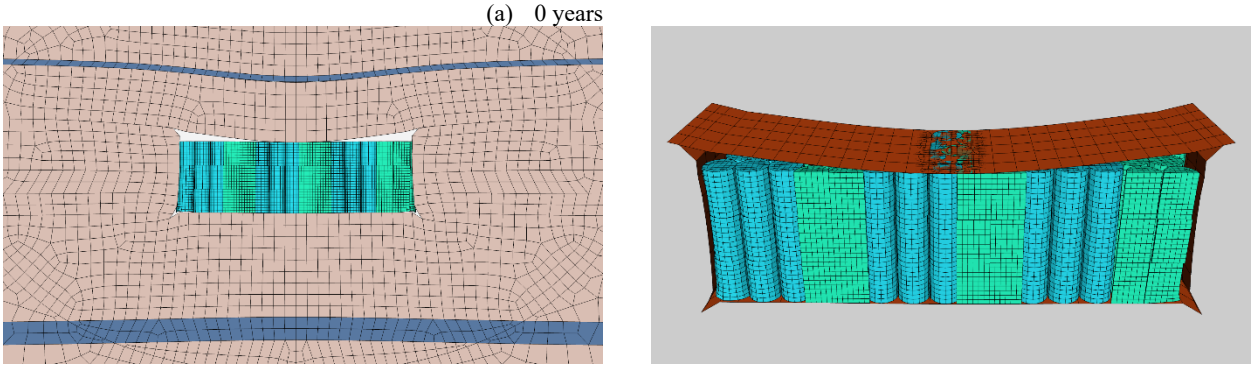

(b) 30 years

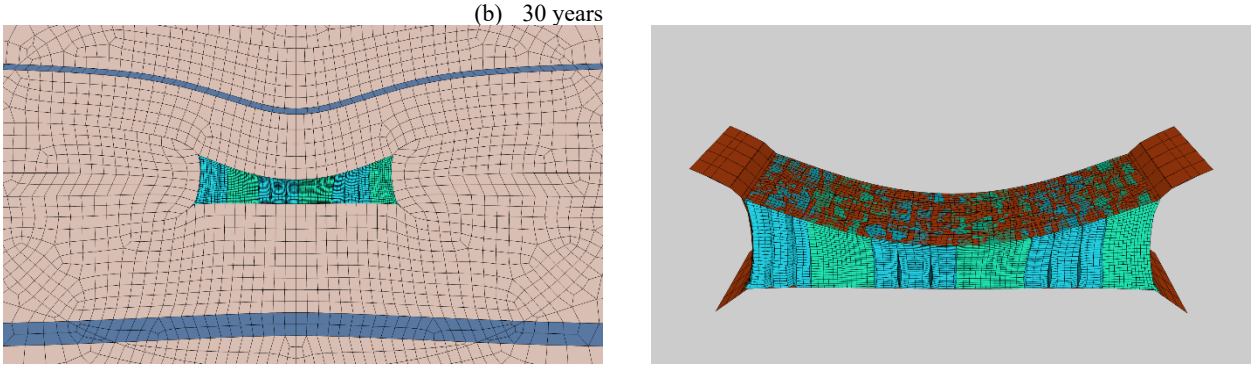

(c) 300 years

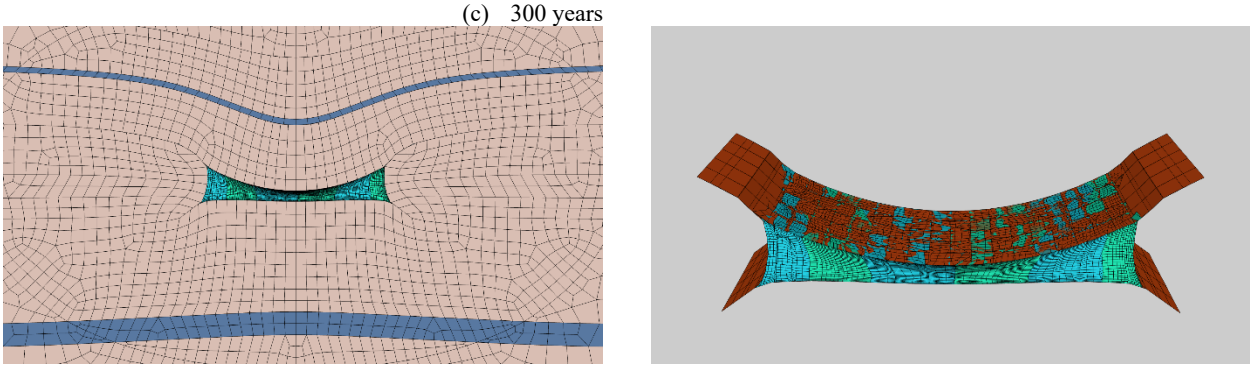

(d) 3000 years

Fig. 28. Deformation of disposal room with 55-gallons drums emplaced as hexagonal array in upper horizon closed by salt creep;[63, Fig. 3-16] thin shelled drums of carbon steel, which quickly shell buckle and shear, are removed as simulation progresses.

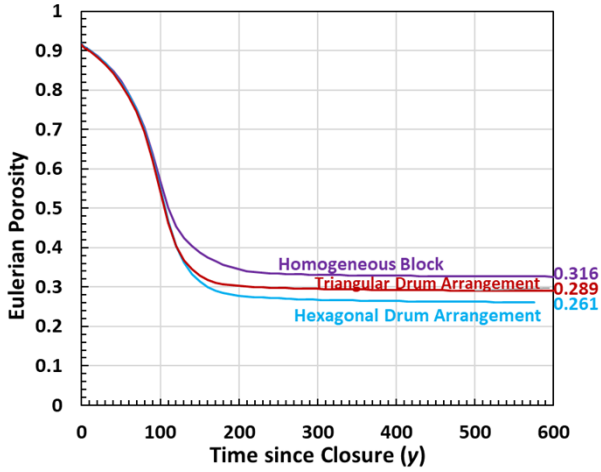

Fig. 29. Eulerian porosity when represented as homogeneous block and hexagonal/triangular arrangements of discrete 55-gallon drums in room segment in upper horizon closed by salt creep without gas generation.[63, Fig. 3-15]

VI.B. Comparison with Asymptotic Critical Concentration when Drums Compacted

The compacted ^{239}Pu fissile concentration is also less than the critical asymptotic concentration for a homogeneous mixture. To elaborate, the initial ^{239}Pu density in a drum with maximum ^{239}Pu is 0.93 kg/m^3 in 0.216 m^3 (internal volume of 55-gallon drum—Table III) for ^{239}Pu uniformly dispersed throughout the waste. Room closure could mechanically compact the uniformly dispersed waste in a drum with maximum fissile content to a higher ^{239}Pu concentration of 3.9 kg/m^3 (i.e., 4.2•0.93 kg/m^3 where the factor 4.2 is based on the density increase discussed in §VI.A.2 above).

The ^{239}Pu concentration of 3.9 kg/m^3 in the assembly is less than the asymptotic critical concentrations of various homogeneous materials that would be present in the 55-gallon drums such as iron, cellulose, salt, and polyethylene plastic (Table II). For example, corroded iron in steel would likely be mixed with ^{239}Pu; yet, the ^{239}Pu concentration of 3.9 kg/m^3 is less than the critical asymptotic concentration of 24.8 kg/m^3 for iron rust. The ^{239}Pu concentration of 3.9 kg/m^3 is also less than the critical asymptotic concentration of 13.2 kg/m^3 for concrete, or 9.1 kg/m^3 for cellulose in Salado brine (Fig. 30). Even if polyethylene plastic filled the 55-gallon drum (and Salado brine did not enter the 20% porosity), the ^{239}Pu concentration of 3.9 kg/m^3 is less than the critical asymptotic concentration for polyethylene of 8.5 kg/m^3 (Fig. 22).

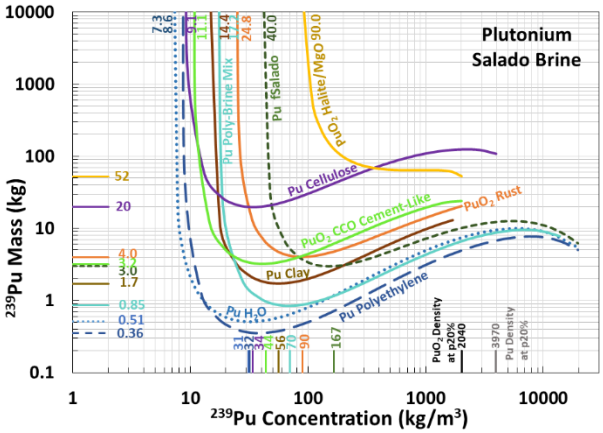

Fig. 30. Critical limits for plutonium mixed with materials potentially present near 55-gallon drums at 20% porosity saturated with Salado brine.[12, Fig. 35;14, Fig. 28]).

VI.C. Standard CH-TRU Drum Behavior Bounded by POCs

The behavior of 6-inch POCs likely bounds standard CH-TRU drum behavior because of three reasons. First, both containers do not provide much resistance to room closure from salt creep (i.e., horizontal closure is the same and vertical closure with 6-inch POCs is 95.5%–Fig. 16) and, thus, each allows for maximum container compaction.

Second, the fissile concentration in CH-TRU drums is much less than in POCs. Specifically, the initial 0.93 kg/m^3 fissile concentration of 0.2 kg ^{239}Pu per one 55-gallon drum with 0.216 m^3 internal volume (Table III) is much less than initial 16.7 kg/m^3 fissile concentration in the 6-inch POC of 0.2 kg ^{239}Pu per POCs with 0.012 m^3 internal volume (Table III). Looking at the configuration in another way, the 9.8-kg/m^3 fissile concentration of a sphere constrained by the inside diameter of a 6-inch POC is much greater than the 2-kg/m^3 Pu concentration of a sphere constrained by the inside diameter of a 55-gallon drum.

Third, total fissile mass in a room full of CH-TRU drums is less than the total fissile mass in a room full of POCs.[n] Specifically, the 1400 FGE ^{239}Pu transportation limit for a 7-pack of 6-inch POCs is 77% greater than the 325 FGE ^{239}Pu transportation limit for a 7-pack of 55-gallon drums in the transportation containers (HalfPACT or TRUPACT-II) (Table IV). Hence, replacing 6-inch POCs in a room with CH-TRU 55-gallon drums, which have the same areal footprint (Table III and Fig. 7), will reduce room reactivity.

[n] To ship a single 55-gallon drum at the maximum 200 FGE would require 1 drum at 125 FGE and 5 dunnage drums in a 7-pack for TRUPACT-II (§II.B.2). To avoid operational concerns, dunnage drums are not removed when disposing a single drum at the maximum 200 FGE limit. Even if this operating procedure was violated, it is improbable that many of the 6804 55-gallon drums necessary to fill a room segment would violate this procedure.

VI.C. Fissile Concentration Less in Large Drums and Containers

A similar rationale applies to larger drums (i.e., 85-gallon with 1.33 m^3 volume and 100-gallon drums with 1.15 m^3—Table III), which have the same transportation limit of 325 FGE ^{239}Pu in 4- and 3-packs of containers. Replacing 6-inch POCs in a room with CH-TRU 85- and 100-gallon drums, which have a similar areal footprint (Table III and Fig. 7), will certainly reduce room reactivity.

Larger drums and very large containers also have a much smaller initial fissile concentration than the 2400 g/m^3 of the 6-inch POC since the transportation limit is still 325 FGE ^{239}Pu per container. The initial concentration over the areal footprint for the 85-gallon and 100-gallon drums is 0.160 kg/m^3 and 0.130 kg/m^3, respectively. The standard waste box (1.88 m^3—Table III), large standard waste box (7.38 m^3), and the 10-drum overpack (2.16 m^3) have initial concentrations of 0.170 kg/m^3, 0.044 kg/m^3, 0.150 kg/m^3, respectively.

The 100-gallon drums with super compacted waste and the very large containers will also compact less than 6-inch POCs, as demonstrated by the difference in compaction from 6-inch POCs and 12-inch POCs (Fig. 14). Hence, the room reactivity will be further reduced, as in Fig. 25. Consequently, criticality is not possible when compacting large CH-TRU waste containers.

VI.D. Neutronic Isolation of RH-TRU Canisters Placed in Room Wall

As noted in §III.D.6, 2005 containers in 719 RH-TRU payload canisters (i.e., often 3 handling containers per canister) have been placed in room walls at WIPP as of April 2019. The 0.66-m diameter canisters are emplaced in 0.7 m diameter boreholes spaced 2.4 m apart centerline to centerline (Fig. 8 and Fig. 31a).

The 2.4 spacing (with 1.7 m of salt) is sufficient to neutronically isolate the canisters from each other; thus, they do not function as a heterogeneous array (Fig. 31b). Hence, the canister fissile mass limits are sufficient to prevent criticality. That is, the canister content is limited to 315 FGE ^{239}Pu without ^{240}Pu (Table V), which is <3.3 kg when optimally moderated Castile brine, <0.52 kg when optimally moderated in water, and <0.47 kg when optimally moderated in water/polyethylene mixture at 3:1 ratio (Fig. 23).

Similarly, the interstitial salt between containers and especially the salt between the left and right sides of a disposal room after 1000 year of creep closure greatly diminishes neutron communication (Fig. 16 and Fig. 19). As noted earlier, the radial distance for defining the POC concentration relates to this neutron communication. Neutron flux has decreased by almost 4 orders of magnitude by 75 cm.

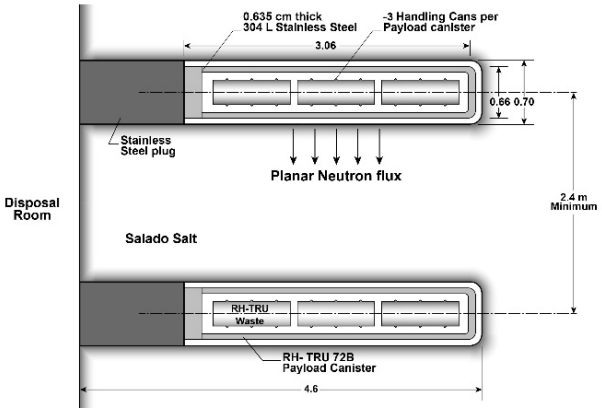

(a) Conceptual model

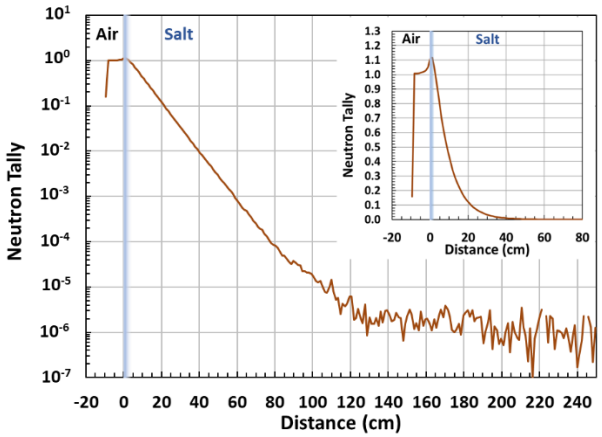

(b) Canister isolation provided by salt

Fig. 31. Neutron communication between RH-TRU payload canisters emplaced horizontally in salt with contents modeled as 1-D planar neutron source in MCNP and absorption by stainless-steel payload canister omitted. 15, Fig. 28

VI.E. RH-TRU Shielded Container Behavior Bounded by POCs

The 2.54 cm of lead and 0.794 cm of carbon steel in shielded containers with RH-TRU (Fig. 32a) is sufficient to drop the surface exposure dose from γ radiation such that the drums can be handled directly by humans similar to other CH-TRU drums; however, 35% of neutrons are able to penetrate the lead (Fig. 32b). Thus, an array of shielded containers disposed in a disposal room is not neutronically isolated by the lead shielding. However, operational concerns prevent the formation of an array after compaction, since shielded containers must be emplaced near room walls and in no more than two tiers (Fig. 7).

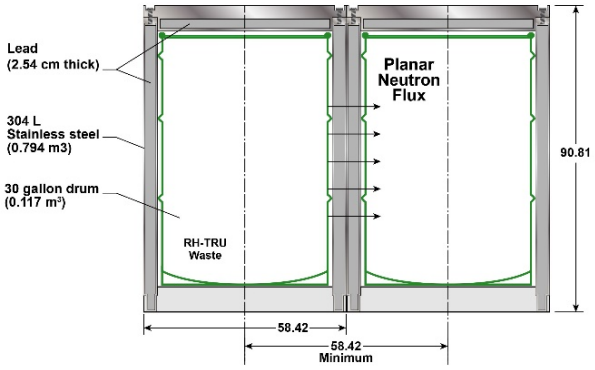

(a) Conceptual model

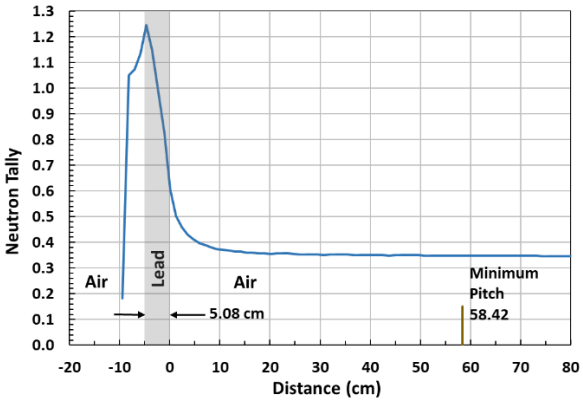

(b) Neutron flux reduced only 65%

Fig. 32. Neutron communication between RH-TRU shielded containers emplaced in disposal rooms with contents modeled as 1-D planar neutron source in MCNP when neutron absorption by carbon-steel drum omitted.[15, Fig. 29]

Furthermore, the behavior of 12-inch POCs, bounds the behavior of the RH-TRU shielded container because the reactivity of the 12-inch POCs is greater that the activity of RH-TRU shielded containers. Specifically, the fissile mass of 1400 FGE ^{239}Pu in the POC 7-pack is 77% greater than 325 FGE ^{239}Pu in the container 3-pack and the initial 4 100-g/m^3 fissile concentration in one 12-inch POC is greater than the maximum 1709-g/m^3 fissile concentration in a shielded container, each with 200 FGE ^{239}Pu—Table III). Yet, the shielded containers would compact similarly to the 12-inch POCs because (a) the footprint of a POC 7-pack is similar to the shielded container 3-pack (3.52 m^2 versus 3.31 m^2–Table III); and (b) both containers are structurally stiff with similar dimensions.

VII. SUMMARY OF LOW-PROBABILITY OF CRITICALITY IN COMPACTED CONTAINERS

Room closure from salt creep at WIPP beneficially encapsulates and isolates TRU waste as containers lose structural integrity; however, the spacing between fissile material in containers is not maintained, which influences the potential for criticality. Herein, the probability of criticality from container compaction after WIPP closure is notionally conceived as the sum of the probability of salt-creep sufficiently compacting three categories of containers disposing TRU waste: (1) pipe overpack containers, (2) drum and box containers, and (3) canisters and shielded containers, where the first two categories are for CH-TRU waste, and the last category is for RH TRU waste. The probability of criticality from compaction is very low for these three categories because criticality cannot occur for a representative salt-creep compaction calculation with bounding fissile loading in the container and reasonable estimates of material present in and about the container, as summarized below.

Criticality has not been included in the CRA-2019 and CRA-2026 WIPP performance assessments[7, App. SCR-2019] based on combining this rationale with the rationale that (1) hydrologic and geochemical conditions cannot sufficiently concentrate ^{239}Pu and ^{235}U elsewhere within the WIPP disposal system; and (2) CCOs cannot go critical when constraints are placed on the mass of hydrogenous material (primarily, plastics) present with the fissile ^{239}Pu in the container or a neutron poison, such as B_4C, is included, as presented in companion reports.[9;10]

VII.A. Constraints on POC Criticality

VII.A.1. Roof Fall in Room Filled with POCs

In simulations of roof-fall, a rigid, trapezoidal, salt block bounces slightly and settles on top of an array of 6-inch or 12-inch POCs without noticeably causing collapse or clustering (Fig. 12). Consequently, large salt falls shortly after WIPP closure are not likely to produce critical assemblies of POCs prior to full room closure from salt creep.

VII.A.2. Closure of Room Filled with POCs

High-fidelity geomechanical simulations were conducted of a room filled with discrete POCs to predict a representative final configuration after room closure from salt creep. Although the integrity of the stainless-steel inner container of POCs could remain for a prolonged period, the 15 MPa lithostatic pressure from salt creep easily buckles the containers or topples them over shortly after the room ceiling contacts the POCs in the simulations. Buckling/toppling allows the POCs to slide past each other such that containers in upper layers are thrust into the bottom layer. The room continues to close until ~1000 years, at which time the 12-in POCs are still mostly upright in two layers in the room center. In contrast, more 6-in POCs are on their side and a single layer has formed in the room center by 1000 years (Fig. 14). The final coordinate positions of POC centroids in

the deformed, irregular array are used in subsequent criticality calculations.

VII.A.3. Material around POCs as Disposal Room Evolves over 10 000 Years

Because spacing is so important, the maximum opportunity for criticality occurs at maximum room closure from salt creep. Yet, criticality evaluation shows that a maximally compacted array of POCs is not critical when material in and around the container is included for (1) room closure with no brine present; (2) a transitional hydrologic regime with influx of some brine to partially saturate pores and initiate metal corrosion and cellulose degradation; and (3) a final hydrologic regime with the influx of more brine that fully saturates containers to complete metal corrosion and cellulose degradation.

VII.A.4. Fiberboard and Iron Isolates POCs in Dry Repository

Maximum room closure from salt creep occurs when gas is not generated from microbial degradation of organics (primarily from cellulose and some plastics and rubber) and container metal corrosion. In turn, no degradation implies that the general integrity of the inner stainless pipe is maintained and fiberboard (cellulose) impact absorber in the POC remains. As with any material that separates the POCs, the fiberboard provides neutronic isolation between containers, even when it is compacted. Similarly, the iron in the inner stainless pipe absorbs some neutrons and the general integrity of the pipe limits the size of fissile material shapes. A deformed array of 12-inch POCs is subcritical ($k_{eff} < 0.91$) (Table VIII). The 6-inch POC is also subcritical; however, it poses a unique situation. An optimally moderated sphere cannot fit inside a 6-inch pipe that maintains its integrity in the first 2000 years; but a deformed, irregular array of optimally moderated 6-inch cylindrical POCs is still subcritical ($k_{eff} < 0.92$) (Fig. 25 and Table VIII).

VII.A.5. Mixing 6-inch and 12-inch POCs

The reduction in k_{eff} between the 6-inch POC and the 12-inch POC remains consistent for the 3 hydrologic regimes (Fig. 27). The reduction in k_{eff} is due to the reduced deformation of the 12-inch POCs as measured by room closure, distance between nearest neighbors, and the distribution of POC concentration. Consequently, if a 7-pack of 12-inch POCs replaces a 7-pack of 6-inch POCs in a disposal room full of 6-inch POCs (with each 7-pack at the maximum fissile content of 1400 FGE ^{239}Pu —Table IV), the room k_{eff} will likely decrease proportional to the number of 6-inch and 12-inch 7-pack POCs because the footprints, heights, and maximum fissile content are identical.

VII.A.6. Brine, Iron, and Fiberboard Isolates Degraded POCs

A compacted array of POCs becomes less reactive when brine enters a fully compacted disposal room even after some microbial degradation of the fiberboard occurs. Specifically, a deformed array of 6-inch POCs has $k_{eff} < 0.90$. A deformed array of 12-inch POCs has $k_{eff} < 0.85$ (Fig. 27 and Table VIII).

VII.A.7. Brine Absorbes Neutrons in Fissile Region of POCs

A compacted array of POCs is not critical when brine mixes with the ^{239}Pu contents as would occur after full degradation of POC and fiberboard (possibly after inadvertent human intrusion) sometime before the end of the 10 000-year regulatory period. Specifically, an analysis of a deformed array of 6-inch POCs is far from critical ($k_{eff} < 0.40$) (Fig. 27 and Table VIII). A deformed array of 12-inch POC is also far from critical ($k_{eff} < 0.35$). Hence, criticality will not occur in a room full of POCs from compaction, especially if brine is present.

VII.B. Insufficient Compaction of Pu in Waste Drums and Boxes

VII.B.1. Low Pu Concentrations in Standard Waste Drums

Standard CH-TRU waste consists of a variety of debris contaminated with TRU radionuclides. The reactivity of 6-inch (or 12-inch) POCs likely bounds standard CH-TRU drum reactivity because (a) the 1400 FGE ^{239}Pu transportation limit in a 7-pack of 6-inch POCs is 77% greater than the 325 FGE ^{239}Pu transportation limit in 7-pack (in a HalfPACT), or 14-pack (in TRUPACT-II—Table IV) of 55-gallon drums or shielded containers; and (b) the 3.5-m^2 disposal footprint of a 7-pack of 6-inch POCs is identical to that of 55-gallon drums (Table III and Fig. 7). Replacing one or all 6-inch POCs with 55-gallon drums will reduce room reactivity (Table VIII).

VII.B.2. Low Pu Concentrations in Larger Drums and Standard Boxes

A similar rationale applies to larger drums (such as 85- and 100-gallon drums), which have a similar footprint (Fig. 7) and same transportation limit of 325 FGE ^{239}Pu (Table IV); thus, the room reactivity will certainly be less than for 6-inch POCs. Furthermore, room reactivity will be less than for 55-gallon drums because (1) the initial fissile concentration is smaller in larger drums, and (2) the larger volume (i.e., 0.315 m^3 for 85-gallon and 0.385 m^3 for 100-gallon drums) (Table III). Similarly, the initial fissile concentration is smaller for large containers (such as standard waste box, large box, or ten drum overpack), and the final fissile density also less for the larger drums and boxes, as demonstrated

by the difference in compaction from 6-inch POCs and 12-inch POCs (Fig. 14).

VII.C. Salt Isolates RH-TRU Canisters

The RH-TRU payload canister, which can contain up to 370 FGE ^{239}Pu has been demonstrated to be subcritical during transportation normal and accident conditions for NRC (Table V). After emplaced in disposal room walls, payload canisters are isolated neutronically by the 1.7 m of salt (2.4 m centerline spacing) between boreholes (Fig. 31). Hence, disposed payload canisters do not act as an array and remain subcritical.

VII.D. POC Behavior Bounds Shielded Container Behavior

The behavior of 12-inch POCs bounds the behavior of RH-TRU shielded containers because 12-inch POC room reactivity is greater than shielded container reactivity because (1) the transportation fissile mass limit of 1400 FGE 239Pu for the 7-pack POC is 77% greater than 325 FGE 239Pu limit for the 3-pack of the shielded container (Table IV), and (2) both containers will compact similarly from room closure from salt creep because both containers are of similar stiffness, size, and footprint (3.5 m2 versus 3.3 m2—Table IV and Fig. 7). Hence, replacing one or all 12-inch in a room with RH-TRU shielded containers will reduce room reactivity (Table VIII).

Table VIII. Rationale that rockfall and salt-creep compaction of POC, drums, and boxes in disposal rooms has low probability of causing criticality at WIPP.[15, Table XI]

Feature ***Event*** **Process**	**Rationale that Roof Fall and Salt-Creep Compaction of Disposal Rooms Does Not Promote Criticality in WIPP Containers**
Room/POC ***Undisturbed*** **Roof Fall**	1. *Initial Waste Emplacement in Repository Not Critical* Rectangular array of 6-inch and 12-inch pipe overpack containers (POCs) represented by spheres with 0.2 kg fissile plutonium (^{239}Pu) is subcritical when initially emplaced with a POC centroid pitch spacing of 58 cm (drum diameter) horizontally and 88 cm vertically. 2. *Roof Fall on Emplaced Waste Does Not Cluster Containers(t < 50 y)* A large, rigid salt block that separates from the roof will bounce slightly and settle on top of an emplaced POC array without causing collapse or clustering and, thereby, producing a critical assembly prior to later gradual room closure from salt creep.
Salt Creep	**Fiberboard and Iron Isolates Pipe Overpack Containers while Repository Dry** 1. *Compacted Array in Repository for Undisturbed Conditions without Brine Influx (t < 1000 y)* For salt compacted array of POCs that is represented with (a) spheres, (b) sphere pitch calculated from salt-creep modeling, (c) sphere diameter constrained by nearest neighbor, (d) 200-g ^{239}Pu contents moderated by water and polyethylene in 3 to 1 ratio, (e) stainless-steel reflection in surrounding region, and (f) 60% of fiberboard (cellulose) reflection (assuming maximum microbial cellulose degradation): i. 6-inch deformed array is subcritical (k_{eff} < 0.92) ii. 12-inch deformed array is subcritical (k_{eff} < 0.91) **2.** For a mixture of 6-inch and 12-inch POCs, room reactivity will reduce proportional to number of 6-inch POCs replaced with 12-inch POCs, because fissile content, height, and footprint are identical.
Salt Creep Brine Influx	**Brine and Iron in Pipe Overpacks Reduces Reactivity when Repository Later Saturated** *Compacted Array in Repository for Undisturbed Conditions with some Brine Influx (1000 y < t < 2000 y)* For compacted array of POCs represented with same conditions as without brine except (a) 20% of interstitial porosity between POCs filled with Castile brine as disposal room transitions from dry to some brine that supports microbially degradation such that (b) 40% of fiberboard reflection remains, and (c) MgO is present in the interstitial porosity: i. 6-inch deformed array is less critical (k_{eff} < 0.90) ii. 12-inch deformed array is less critical (k_{eff} < 0.85)
Undisturbed/ Disturbed **Brine Inundation**	*Compacted Array for Undisturbed/Disturbed Conditions with Brine Inundation (t >2000 y)* For compacted array of POCs represented with same conditions as with above except (a) no fiberboard remains, (b) 200-FGE ^{239}Pu region moderated by Castile brine and plastics in 3 to 1 ratio, and (c) iron, magnesium oxide, and salt reflection in surrounding region: i. 6-inch deformed array is much less critical (k_{eff} < 0.40) ii. 12-inch deformed array is much less critical (k_{eff} < 0.36)
Room/ CH Drums & Boxes ***Undisturbed*** **Salt Creep**	**Insufficient Compaction of Low Fissile Concentration in Waste Drums and Boxes** 1. The behavior of 6-inch POCs likely bounds standard CH-TRU drum behavior because (1) the 1400-FGE ^{239}Pu transportation limit in the 6-inch POCs is 77% greater than 325 FGE ^{239}Pu for 7-pack of 55-gallon drums, each with the same footprint (3.5 m^2); (2) both containers are structurally weak and, thus, allow for maximum room closure; and (3) the Pu initial concentration of 16.7 kg/m^3 for 6-inch POC is much greater than 0.93 kg/m^3 for waste drum (where each container contains 200-FGE ^{239}Pu, is bound by the inner container diameter—Table III). Hence, replacing 7-pack of 6-inch POCs with 7-pack of 55-gallon CH-TRU drums will reduce room reactivity. 2. A similar rationale applies to larger drums and boxes, which all have a similar footprint and same transportation limit of 325 FGE ^{239}Pu; thus, the room reactivity will be less than for 6-inch POCs.
Room/ RH Canisters & RH Shielded Containers ***Undisturbed*** **Salt Creep**	**Salt Isolates RH-TRU Canisters and POC Behavior Bounds Shielded Container Behavior** 1. RH-TRU canisters disposed in room walls are neutronically isolated by 1.7 m of salt between boreholes. 2. Behavior of 12-inch POCs bounds behavior of RH-TRU shielded containers because 12-inch POC room reactivity is greater than shielded container since the transportation fissile mass limit of 1400 FGE ^{239}Pu for the 7-pack POC is 77% greater than 325 FGE ^{239}Pu limit for the 3-pack shielded container; yet, both containers will compact similarly from room closure because both containers are of similar size, footprint (3.5 m^2 versus 3.3 m^2); and structurally stiffness. Hence, replacing one or all 12-inch POCs in a room with RH-TRU shielded container will reduce room reactivity.

REFERENCES

[1] R.P. Rechard, L.C. Sanchez, H.R. Trellue, and C.T. Stockman. 2001. Unfavorable conditions for nuclear criticality following disposal of transuranic waste at the Waste Isolation Pilot Plant. *Nuclear Technology,* **136** (1) 99–129.

[2] R.P. Rechard, L.C. Sanchez, C.T. Stockman, and H.R. Trellue. 2000. Consideration of nuclear criticality when disposing of transuranic waste at the Waste Isolation Pilot Plant, SAND99-2898. Albuquerque, NM: Sandia National Laboratories.

[3] R.P. Rechard. 2015. Probability and consequences of nuclear criticality at a geologic repository--I: conceptual overview for screening. *Nuclear Technology,* **190** (2) 97–126.

[4] DOE (US Department of Energy). 2022. Transuranic waste acceptance criteria for the Waste Isolation Pilot Plant, DOE/WIPP-02-3122, Revision 11. Carlsbad, NM: US Department of Energy, Carlsbad Field Office.

[5] DOE (US Department of Energy). 2024. Notice of availability of final environmental impact statement for surplus plutonium disposition program. *Federal Register,* **89** (13) 3642–3644.

[6] NA/NRC (National Academies/National Research Council). 2020. Review of the Department of Energy's plans for disposal of surplus plutonium in the Waste Isolation Pilot Plant, Washington, DC: The National Academies Press.

[7] DOE (US Department of Energy). 2019. Title 40 CFR Part 191 Compliance Recertification Application for the Waste Isolation Pilot Plant, DOE/WIPP-10-3609. Carlsbad, NM: Carlsbad Area Office, US Department of Energy.

[8] R.P. Rechard, B.A. Day, B. Reedlunn, and J.E. Bean, Jr. 2025. Improbability of post-closure criticality in compacted criticality control overpacks after room closure at Waste Isolation Pilot Plant, SAND2025. Albuquerque, NM: Sandia National Laboratories.

[9] R.P. Rechard, B.A. Day, B. Reedlunn, and J.E. Bean, Jr. 2022. Improbability of nuclear criticality in criticality control overpacks after salt creep compaction at Waste Isolation Pilot Plant, SAND2022-0952. Albuquerque, NM: Sandia National Laboratories.

[10] R.P. Rechard, S. King, and P.V. Brady. 2025. Hydrologic and geochemical constraints on post-closure criticality in geologic media near Waste Isolation Pilot Plant, SAND2025. Albuquerque, NM: Sandia National Laboratories.

[11] R.P. Rechard. 2025. Low risk of post-closure criticality at Waste Isolation Pilot Plant SAND2025. Albuquerque, NM: Sandia National Laboratories.

[12] R.P. Rechard. 2025. Fissile mass and concentration necessary for post-closure criticality in geologic media near bedded salt repository Memorandum to Steve Wagner, 8880; Ross Kirkes, 8883; October 2025, ERMS. Albuquerque, NM: Sandia National Laboratories.

[13] R.P. Rechard, L.C. Sanchez, P.J. McDaniel, J. Hunt, and G. Broadous, Fissile mass and concentration criteria in geologic media near bedded salt repository presented at the International High-Level Radioactive Waste Management Conference, April 14-18, 2019, Knoxville, TN, 2019.

[14] R.P. Rechard, L.C. Sanchez, M. Olgvun, and G. Ryba. 2019. Fissile mass and concentration necessary for criticality in geologic media near bedded salt repository, Memorandum to Paul E. Shoemaker, 8880; Todd Zeitler, 8862; Ross Kirkes, 8883; November 2019, Albuquerque, NM: Sandia National Laboratory.

[15] R.P. Rechard. 2019. Improbability of transuranic waste compaction by salt creep causing criticality in bedded salt repository; Memorandum to Paul E. Shoemaker, 8880; Todd Zeitler, 8863; Ross Kirkes, 8883; November 2019, Albuquerque, NM: Sandia National Laboratories.

[16] EPA (US Environmental Protection Agency). 1985. 40 CFR Part 191: Environmental standards for the management and disposal of spent nuclear fuel, high-level and transuranic radioactive wastes: final rule. *Federal Register,* **50** (182) No. 182, 38066–38089.

[17] EPA (US Environmental Protection Agency). 1993. 40 CFR Part 191: Environmental radiation protection standards for the management and disposal of spent nuclear fuel, high-level and transuranic radioactive wastes, final rule. *Federal Register,* **58** (242) 66398–66416.

[18] R.P. Rechard. 2000. Historical background on performance assessment for the Waste Isolation Pilot Plant. *Reliability Engineering and System Safety,* **69** (1-3) 5–46.

[19] S. Kaplan and B.J. Garrick. 1981. On the quantitative definition of risk. *Risk Analysis,* **1** (1) 11–27.

[20] NRC (US Nuclear Regulatory Commission). 2003. Yucca Mountain review plan, final report, NUREG-1804, REV 2. Washington, DC: Office of Nuclear Material Safety and Safeguards, US Nuclear Regulatory Commission.

[21] EPA (US Environmental Protection Agency). 1996. 40 CFR Part 194: Criteria for the certification and re-certification of the Waste Isolation Pilot Plant's compliance with the 40 CFR Part 191 disposal regulations; final rule. *Federal Register,* **61** (28) 5224–5245.

[22] P. Vaughn, J.E. Bean, J.C. Helton, M.E. Lord, R.J. MacKinnon, and J.D. Schreiber. 2000. Representation of two-phase flow in the vicinity of the repository in the 1996 performance assessment for the Waste Isolation Pilot Plant. *Reliability Engineering and System Safety,* **69** (1-3) 205–226.

[23] B. Reedlunn and J.E. Bean, Jr. 2019. Simulations of pipe overpack container compaction at the Waste Isolation Pilot Plant SAND2019-12111. Albuquerque, NM: Sandia National Laboratories.

[24] C.M. Stone. 1997. Final disposal room structural response calculations, SAND97-0795. Albuquerque, NM: Sandia National Laboratories.

[25] Pub. L. 102-579. 1992. *Waste Isolation Pilot Plant Land Withdrawal Act*, 106 Stat. 4777.

[26] R.P. Rechard. 2000. Milestones for disposal of radioactive waste at the Waste Isolation Pilot Plant (WIPP) in the

United States, SAND98-0072, Revised. Albuquerque, NM: Sandia National Laboratories.

[27] US Courts. 1981. State of New Mexico, ex rel., Jeff Bingaman, Attorney General of the State of New Mexico, Plaintiff, v. The United States Department of Energy, et al., Defendants, 1981. "Stipulated Agreement." Civil Action No. 81-0363 JB. July 1, 1981, United States District Court for the District of New Mexico.

[28] DOE (US Department of Energy). 1996. Final programmatic environmental impact statement, EIS-0229. Washington, DC: US Department of Energy.

[29] DOE (US Department of Energy). 2007. Notice of intent to prepare a supplemental environmental impact statement for surplus plutonium disposition at the Savannah River Site. *Federal Register,* **72** (59) 14543–14546.

[30] DOE (US Department of Energy). 2008. Yucca Mountain repository license application, safety analysis report, DOE/RW-0573, Rev. 1. Washington, DC: Office of Civilian Radioactive Waste Management, US Department of Energy.

[31] DOE (US Department of Energy). 2012. Draft surplus plutonium disposition supplemental environmental impact statement, DOE/EIS-0283-S2. Washington, DC: Office of Environmental Managment, US Department of Energy.

[32] DOE (US Department of Energy). 2016. Surplus plutonium disposition, record of decision. *Federal Register,* **81** (65) 19588–19594.

[33] DOE (US Department of Energy). 2024. Record of decision for the final Environmental Impact Statement for the Surplus Plutonium Disposition Program. *Federal Register,* **89** (77) 28763–28767.

[34] DOE (US Department of Energy). 1996. Title 40 CFR Part 191: Compliance certification application for the Waste Isolation Pilot Plant, DOE/CAO-1996-2184. Vol. I-XXI. Carlsbad, NM: DOE Carlsbad Area Office.

[35] R.J. MacKinnon, G.A. Freeze, and H. Jow. 1997. Summary of EPA-mandated performance assessment verfication test (replicate 1) and cmoparison with the compliance certificatin application calculations, revision 1, ERMS 541521. Carlsbad, NM: Sandia National Laboratories.

[36] DOE (US Department of Energy). 2004. Title 40 CFR Part 191: Compliance recertification application for the Waste Isolation Pilot Plant, DOE/WIPP 2004-3231. Carlsbad, NM: Waste Isolation Pilot Plant, Carlsbad Field Office, US Department of Energy.

[37] C.D. Leigh, J. Trone, and B. Fox. 2005. TRU waste inventory for the 2004 compliance recertification application performance assessment baseline calculation, ERMS 541118. Carlsbad, NM: Sandia National Laboratories.

[38] B. Crawford, D. Guerin, S. Lott, W. McInroy, J. McTaggart, and G.D. Van Soest. 2009. Performance assessment inventory report - 2008, INV-PA-08, Revision 0. Carlsbad, NM: Los Alamos National Laboratory, Carlsbad Operations.

[39] D.J. Clayton, S.C. Dunagan, J.W. Garner, A.E. Ismail, T.B. Kirchner, G.R. Kirkes, and M.B. Nemer. 2008. Summary report of the 2009 compliance recertification application performance assessment, ERMS 548862. Carlsbad, NM: Sandia National Laboratories.

[40] D.J. Clayton, R.C. Camphouse, J.W. Garner, A.E. Ismail, T.B. Kirchner, K.L. Kuhlman, and M.B. Nemer. 2010. Summary report of the CRA-2009 performance assessment baseline calculation, ERMS 559466. Carlsbad, NM: Sandia National Laboratories.

[41] G.D. Van Soest. 2012. Performance assessment inventory report - 2012, INV-PA-12, Rev. 0; LA-UR-12-26643. Carlsbad, NM: Los Alamos National Laboratory Carlsbad Operations.

[42] G.D. Van Soest. 2018. Performance assessment inventory report - 2018, INV-PA-18, Revision 0. Carlsbad, NM: Los Alamos National Laboratory.

[43] G.D. Van Soest. 2025. Full repository performance assessment inventory report - 2024, INV-FPA-24. Carlsbad, NM: Los Alamos National Laboratory.

[44] H.K. Clark. 1981. Subcritical limits for plutonium systems. *Nuclear Science and Engineering,* **79** (1) 65–84, doi: 10.13182/NSE81-A19043.

[45] ANSI (American National Standards Institute). 2014. An American national standard for nuclear criticality safety in operations with fissionable materials outside reactors, ANSI/ANS-8.1-2014. La Grange Park, IL: American National Standards Institute.

[46] NRC (US Nuclear Regulatory Commission). 2020. Certificate of complicance for radioactive material packages, TRUPACT-II, Certificate 9218, Rev 25, Docket 71-9218. Washington, DC: US Nuclear Regulatory Commission.

[47] NRC (US Nuclear Regulatory Commission). 2020. Certificate of compliance for radioactive material packages, HalfPACT waste shipping container, Certificate 9279, Rev. 9, Docket 71-9279. Washington, DC: US Nuclear Regulatory Commission.

[48] NRC (US Nuclear Regulatory Commission). 2019. Certificate of compliance for radioactive material package RH-TRU 72-B, Revision 11, Docket 71-9212. Washington DC: US Nuclear Regulatory Commission.

[49] DOE (US Department of Energy). 2015. RH-TRU 72-B safety analysis report, Revision 7. Carlsbad, NM: US Department of Energy, Carlsbad Area Field Office.

[50] DOE (US Department of Energy). 2018. Transuranic waste acceptance criteria for the Waste Isolation Pilot Plant, DOE/WIPP-02-3122, Rev. 9. Carlsbad, NM: Carlsbad Field Office, US Department of Energy.

[51] NWP (Nuclear Waste Partnership). 2021. Nuclear criticality safety evaluation for contact-handled transuranic waste containers at the Waste Isolation Pilot Plant, WIPP-016, Revision 6. Carlsbad, NM: Nuclear Waste Partnership.

[52] B.A. Day. 2013. Calculation of CH and RH payload container waste volumes, PLD-CAL-0001, Rev. 1. Carlsbad, NM: Nuclear Waste Partnership.

[53] DOE (US Department of Energy). 2022. CH-TRAMPAC, Revision 6. Carlsbad, NM: Carlsbad Field Office, US Department of Energy.

[54] B.Y. Park and F.D. Hansen. 2005. Determination of the porosity surfaces of the disposal room containing various waste inventories for WIPP PA, SAND2005-4236. Albuquerque, NM: Sandia National Laboratories

[55] G.R. Kirkes. 2019. "POC data as of June 1 2019.xlsx" Excel spreadsheet showing all emplaced pipe overpack containers, emplacement location, and waste information as of June 1, 2019., ERMS 571584. Carlsbad, NM: Sandia National Laboratories.

[56] DOE (US Department of Energy). 2015. RH-TRAMPAC, Revision 3. Carlsbad, NM: Carlsbad Field Office, US Department of Energy.

[57] R.P. Rechard, A.C. Peterson, J.D. Schreiber, H.J. Iuzzolino, M.S. Tierney, and J.S. Sandha. 1991. Preliminary comparison with 40 CFR Part 191, Subpart B for the Waste Isolation Pilot Plant, December 1991, Volume 3: Reference Data, SAND91-0893/3. Albuquerque, NM: Sandia National Laboratories

[58] DOE (US Department of Energy). 2014. Title 40 CFR Part 191 Subparts B and C Compliance Recertification Application 2014 for the Waste Isolation Pilot Plant, DOE/WIPP-14-3503. Carlsbad, NM: US Department of Energy, Carlsbad Field Office.

[59] Accident Investigation Board and DOE (US Department of Energy). 2014. Radiological release event at the Waste Isolation Pilot Plant on February 14, 2014, Accident Investigation Report, Washington, DC: US Department of Energy, Office of Environmental Management. [Online]. Available: https://wipp.energy.gov/wipprecovery-accident-desc.asp

[60] DOE (US Department of Energy). October 14, 2016, plans call for controlled withdrawal from south end of underground. http://www.wipp.energy.gov/Special/WIPP%20Update%2010_14_16.pdf (accessed.

[61] S. Brunell, J. Bethune, P. Docherty, D.C. Kicker, S. Kim, S. King, J. Long, and T.R. Zeitler. 2023. Summary report for the 2023 replacement panels planned change request performance assessment, ERMS 579729. Carlsbad, NM: Sandia National Laboratories.

[62] J.D. Schreiber. 1991. Updated waste storage volumes, ERMS 236055. Albuquerque, NM: Sandia National Laboratories.

[63] C. Vignes, J.E. Bean, Jr., and B. Reedlunn. 2023. Improved modeling of Waste Isolation Pilot Plant disposal room porosity, SAND2023-04826. Albuquerque, NM: Sandia National Laboratories.

[64] NWP (Nuclear Waste Partnership). 2021. CH waste downloading and emplacement technical procedure, WP 05-WH1025, Rev. 30. Carlsbad, NM: Nuclear Waste Partnership.

[65] Y. Wang and L.H. Brush. 1996. Estimates of gas-generation parameters for the long-term WIPP performance assessment, memorandum to M.S. Tierney, January 26, 1996, ERMS 231943. Albuquerque, NM: Sandia National Laboratories.

[66] Y. Wang and L.H. Brush. 1996. Modify the stoichiometric factor y in the BRAGFLO to include the effect of MgO added to WIPP repository as a backfill, memorandum to M.S. Tierney, February 23, 1996, ERMS 232286. Albuquerque, NM: Sandia National Laboratories.

[67] EPA (US Environmental Protection Agency). 2001. Approval for the elimination of magnesium oxide mini-sacks from the Waste Isolation Pilot Plant. Letter from Frank Marcinowski, EPA to Dr. Ines Triay, DOE, ERMS 519362. Washington, DC:: US Environmental Protection Agency, Office of Radiation and Indoor Air.

[68] J. Reyes. 2008. Letter to D.C. Moody (5 Enclosures). 11 February 2008., ERMS 549331. Washington, DC: US Environmental Protection Agency, Office of Radiation and Indoor Air.

[69] D.E. Munson, A.F. Fossum, and P.E. Senseny. 1989. Advances in resolution of discrepancies between predicted and measured in situ WIPP room closures, SAND88-2948. Albuquerque, NM: Sandia National Laboratories.

[70] B. Reedlunn and J.E. Bean, Jr. 2021. Additional simulations of criticality control overpack and pipe overpack container compaction at the Waste Isolation Pilot Plant SAND2021-11268 CTF. Albuquerque, NM: Sandia National Laboratories.

[71] P.S. Domski. 2023. Prediction of baseline actinide solubilities for the replacement panels planned change request (RPPCR) performance assessment, ERMS 555726. Carlsbad, NM: Sandia National Laboratories.

[72] J.L. Krumhansl, K.M. Kimball, and C.L. Stein. 1991. Intergranular fluid compositions from the Waste Isolation Pilot Plant (WIPP), Southeastern New Mexico, SAND90-584. Albuquerque, NM: Sandia National Laboratories.

[73] R.S. Popielak, R.L. Beauheim, S.R. Black, W.E. Coons, C.T. Ellingson, and R.L. Olsen. 1983. Brine reservoirs in the Castile Formation, Waste Isolation Pilot Plant Project, sourtheastern New Mexico, TME 3153. Carlsbad, NM: U.S. Department of Energy, WIPP Project Office.

[74] DOE (US Department of Energy). 2016. Waste Isolation Pilot Plant documented safety analysis, DOE/WIPP 07-3372. Carlsbad, NM: US Department of Energy, Carlsbad Field Office.

[75] B. Reedlunn and J.E. Bean, Jr. 2020. Further simulations of criticality control overpack container compaction at the Waste Isolation Pilot Plant, memorandum, SAND2020-5105 CTF. Albuquerque, NM: Sandia National Laboratories.

[76] B.M. Butcher, T.W. Thompson, R.G. VanBuskirk, and N.C. Patti. 1991. Mechanical compaction of Waste Isolation Pilot Plant simulated waste, SAND90-1206. Albuquerque, NM: Sandia National Laboratories.

[77] B.M. Butcher. 1997. A summary of the sources of input parameter values for the WIPP final porosity surface calculations, SAND97-0796. Albuquerque, NM: Sandia National Laboratories.

[78] C.M. Stone. 1997. SANTOS - a two-dimensional finite element program for the quasistatic, large deformation, inelastic response of solids, SAND90-0543. Albuquerque, NM: Sandia National Laboratories.

[79] B. Reedlunn, J.G. Arguello, and F.D. Hansen. 2022. A reinvestigation into Munson's model for room closure in bedded rock salt. *International Journal of Rock*

Mechanics and Mining Sciences, **151** 105007, doi: doi.org/10.1016/j.ijmms.2021.105007.

[80] SNL (Sandia National Laboratories). 2018. Sierra/Solid Mechanics user's guide. 4.50, SAND2018-10673. Albuquerque, NM: Sandia National Laboratories.

[81] B. Reedlunn and J.E. Bean, Jr. 2020. Impact of properly specifying the Clay F and Clay G friction coefficients in disposal room closure simulations at the Waste Isolation Pilot Plant. Memorandum, SAND2020-3537 CTF. Albuquerque, NM: Sandia National Laboratories.

[82] B. Reedlunn, G. Moutsanidis, J. Baek, T.-H. Huang, J. Koester, E. Matteo, X. He, K. Taneja, H. Wei, Y. Bazilevs, J.-S. Chen, C. Mitchell, R. Lander, and T. Dewers. 2019. Initial simulations of empty room collapse and reconsolidation at the Waste Isolation Pilot Plant, SAND2019-15351. Albuquerque, NM: Sandia National Laboratories.

[83] B. Reedlunn, G. Moutsanidis, J. Baek, T.-H. Huang, J. Koester, X. He, H. Wei, K. Taneja, Y. Bazilevs, and J.-S. Chen, Initial simulations of empty room collapse and reconsolidation at the Waste Isolation Pilot Plant, presented at the 54th US Rock Mechanics/Geomechanics Symposium 28 June-1 July, Golden, Colorado, 2020, ARMA 20-1590.

[84] B.D. Brickner. 2019. Post-closure nuclear criticality evaluations involving 6- and 12-inch pipe overpack TRU waste containers at the Waste Isolation Pilot Plant, ORNL/TM-2019/1222. Oak Ridge, TN: Oak Ridge National Laboratory.

[85] J.F. Briesmeister. 1986. MCNP--A general Monte Carlo Code for neutron and photon transport LA-7396-M-Rev. 2. Los Alamos, NM: Los Alamos National Laboratory. Most recent version available from Radiation Safety Information Computational Center, Oak Ridge National Laboratory, Oak Ridge, TN.

[86] J.J. Duderstadt and L.J. Hamilton, *Nuclear Ractor Analysis*. New York, NY: John Wiley & Sons, 1976.

[87] R.P. Rechard and M.S. Tierney. 2005. Assignment of probability distributions for parameters in the 1996 performance assessment for the Waste Isolation Pilot Plant, Part 2: Application of process. *Reliability Engineering and System Safety,* **88** (1) 33–80.

[88] R. Jensen, S. Broome, C. Herrick, and B. Reedlunn. 2023. Improved compaction experiments and modeling of Waste Isololation Pilot Plant standard, non-degraded, waste containers, SAND2023-04823. Albuquerque, NM: Sandia National Laboratories.

DISTRIBUTION

E-mail—Internal

Benjamin Reedlunn	01558	breedlu@sandia.gov
James E. Bean, Jr.	01554	jebean@sandia.gov
Emily R. Stein	01864	ergiamb@sandia.gov
Joshua Rutkowski	06817	jerutko@sandia.gov
R. Chris Camphouse	08842	rccamph@sandia.gov
Carmen M Mendez	08844	cmmende@sandia.gov
Brad A. Day	08881	baday@sandia.gov
G. Ross Kirkes	08881	grkirke@sandia.gov
Technical Library	01977	sanddocs@sandia.gov

E-mail—External

Bret D. Brickner	bricknerbd@ornl.gov	Oak Ridge National Laboratory
Riley M. Cumberland	cumberlandrm@ornl.gov	Oak Ridge National Laboratory
Ronald Livingston	ronald.livingston@srs.gov	Omega Technical Services



Sandia National Laboratories

Sandia National Laboratories is a multimission laboratory managed and operated by National Technology & Engineering Solutions of Sandia LLC, a wholly owned subsidiary of Honeywell International Inc. for the U.S. Department of Energy's National Nuclear Security Administration under contract DE-NA0003525.